A TWO-DIMENSIONAL HYDRODYNAMIC MODEL FOR THE ST LUCIA ESTUARY MOUTH

by

Kathryn Margaret Jaaback B.Sc.(Hons.)

Submitted in partial fulfilment of the requirements
for the degree of Master of Science,
in the
Department of Geology and Applied Geology,
University of Natal, Durban
and
Department of Mathematics and Applied Mathematics
University of Natal, Pietermaritzburg

January 1993

ABSTRACT

The reduced fresh water input into the St Lucia Estuary combined with the increase of sediment in the St Lucia Lake System has necessitated the implementation of a dredging programme. To ensure the effectiveness of the dredging programme, the behaviour of the sediment under various flow and tidal conditions needs to be determined.

To establish how sediment will move, it is necessary to understand the hydrodynamics of the estuary. To achieve this, a hydrodynamic model which can be linked to a sediment transport model needs to be developed. Various existing types of hydrodynamic and sediment transport models are reviewed, to determine their suitability for the above purpose. Results of the analysis indicate that a two-dimensional hydrodynamic model is required.

The two-dimensional hydrodynamic model developed is based on the momentum and continuity equations for an unsteady, non-uniform, free-surface flow for an incompressible fluid. The two dimensions are in the horizontal plane and flow is averaged over the depth. The equations are non-linear and are not decoupled, thus a numerical technique was needed to solve them. An Alternating Direction Implicit technique has been used. Boundary conditions in the modelled region were specified as flow velocity at the upstream boundary, and water levels, relative to the Mean Lake Level, at the downstream boundary.

Two short simulations using hypothetical data were run on a 80826 IBM compatible. Results of the simulation indicate two areas where irregularities in the model output are a consequence of the use of hypothetical data in defining the boundary conditions. Recommendations for the collection of data in order to improve and calibrate the model are discussed.

PREFACE

This thesis represents the original work of the author and has not been submitted in any form to another university. Where use has been made of the work of others it has been duly acknowledged in the text.

The project was supervised by Professor T.R. Mason in the Department of Geology and Applied Geology, University of Natal, Durban; and Professor J. Hearne in the Department of Mathematics and Applied Mathematics, University of Natal, Pietermaritzburg.

ACKNOWLEDGEMENTS

I am most grateful for the help of the following people:

My supervisors, Prof. Tom Mason of the Geology and Applied Geology Department, University of Natal, Durban and Prof. John Hearne of the Mathematics and Applied Mathematics Department, University of Natal, Pietermaritzburg.

Natal Parks Board and the University of Natal for providing financial assistance.

My family for keeping me motivated.

CONTENTS

CHAPTER 1

INTRODUCTION

Decisions that have far reaching economical and environmental implications can seldom be made on the basis of intuition alone. This is the problem faced by the Natal Parks Board (NPB), regarding the management of the St Lucia Estuary Mouth. The physical properties of the estuary have been noted since 1918 (Hutchison, 1976) and the impact of changes in the hydrology, topography, meteorology and ecology of the drainage basin have been recorded. These changes can be due to either natural phenomena, for example the floods following cyclone Demonia in 1984; or man's interference such as the separation of the St Lucia and Mfolozi River Mouths which reduced the freshwater input into the St Lucia Lake system. At present these records exist in the form of several scientific papers and aerial photographs. In more recent years NBP personnel have monitored such variables as water levels, salinities and flow discharges. However as the pressures on the estuary increase due to :

(1) its expansion as a recreational resort;

(2) the deterioration of the catchment resulting from poor farming techniques;

(3) the greater demands on water resources and the increased pollution as the town of St Lucia grows;

a more detailed and scientific management approach is required making use of regular monitoring of the predominant variables.

This need for a scientific approach was identified and thus a Joint Venture Programme between the Foundation for Research and Development, the Department of Water Affairs, the Department of Environment Affairs, Portnet and the Natal Provincial Administration, was established to look at the Estuary-Coastal Lake

Systems. The objectives outlined in the research programme were to get a better understanding of how the abiotic and biotic components of and estuary affect the mouth dynamics, and consequently how estuaries should be managed, monitored and utilised.

Some of the questions that arose in the Joint Venture Programme relating to the abiotic components of an estuary were: how fluvial and tidal flushing affect an estuary; what are the consequences of artificially changing river courses; and which options of bank stabilisation are suitable for specific estuaries. To partially answer these questions a hydrodynamic model for estuarine systems needs to be developed.

The aim of this study is to look at the hydrodynamics of estuarine systems, with particular emphasis on the St Lucia estuary system, noting previous observations and studies, and to express the physical processes in a mathematical model. At this stage insufficient data is available for the St Lucia estuary to calibrate a model and to get accurate results. The model will thus only used hypothetical data. Ultimately, although not in this study, the aim is to integrate the fluid dynamic model with a sediment transport model. At this stage several sediment transport models will be reviewed and the constraints under which they operate will be borne in mind when developing the hydrodynamic model.

The purpose of a model is not to describe complex physical processes accurately, but to rather to simplify them so that the relationships between the major influencing factors can be determined. From these relationships predictions can be made as to how the physical processes will behave when these factors are altered. To include all the factors influencing the hydrodynamics of an estuarine system would make a model extremely complex and too cumbersome to computerise. To simplify the process the effects of several variables were assumed to be negligible and these variables were omitted from the model. This process also enhanced computerisation.

To decide which type of hydrodynamic model should be used the flow within an estuary must be examined.

Firstly, looking at a river one can see that the water flows predominantly in the direction parallel to the river banks but secondary movement also occurs across the breadth and depth of a river. In an estuary, flow patterns are similar to a river. However the flow direction is periodically reversed due to the changing tides. The flow is thus *3-dimensional.*

Secondly, due to the fact that the flow in an estuary depends on time variable phenomena such as the tides, the amount of rainfall, the wind velocity, and the depth and gradient of the channel, the flow is continually changing. Hydrodynamically this type of flow is termed *unsteady.*

Thirdly, due to changes in the channel geometry the fluid motion varies according to where it is being observed. This change in flow between different spatial locations is termed *non-uniform.*

Fourthly, water in an estuary is confined by the bed and the banks and the surface is free to rise or fall. In other words flow occurs under a *free-surface.*

Finally, water is assumed to be *incompressible.*

Thus the hydrodynamics of an estuary can be described by setting up *3-dimensional, unsteady, non-uniform, free-surface* flow equations for an *incompressible* fluid.

The hydrodynamic equations are expressed as partial differential equations (PDEs), as fluid motion exists in the continuum of space and the continuum of time. However, the exact solution of these equations is often impossible due to their non-linearity and complexity. To overcome this problem the equations defining the fluid behaviour must be written in discrete terms. This is done by describing the continuous motion by a finite sequence of numbers, which describe the flow at

different spatial locations, and these are transformed by a set of operations to simulate the change in flow as time progresses. There are several numerical methods that can be used to solve these equations: finite difference methods; finite element methods; and the method of characteristics to name but a few. These methods can be further classified into implicit and explicit methods of solution. Each technique will be briefly discussed in Chapter 5.

The steps taken in this thesis to develop a hydrodynamical model based on the St Lucia Estuary Mouth were as follows:

(1) review existing sediment transport models in order to formulate a set of guide lines when developing a hydrodynamical model;

(2) review one-dimensional models which have been previously applied to the St Lucia Estuary Mouth;

(3) derive a system of equations which will describe the hydrodynamics of the estuary, taking boundary and initial conditions into account;

(4) determine which numerical method is best suited to the solution of the hydrodynamic equations while taking into consideration the computer facilities available;

(5) develop a computer program based on the above solution technique using hypothetical data;

(6) note the results of the model using hypothetical data and discuss its shortfalls and recommend further modifications so that the model may become an integral tool for management decision making.

CHAPTER 2

SEDIMENT TRANSPORT

2.1 NOTATION

d	grain diameter of uniform sand	mm
D	grain diameter of uniform sand	m
D_{50}	grain diameter of bed material for which 50% of the grains have a smaller diameter	m
k	inverse of Manning coefficient	$m^{1/3}.s^{-1}$
q_{bv}	transport rate by volume of the bed load per unit width	$m^2.s^{-1}$.
q_{bw}	transport rate by weight of the bed load per unit width	$kg.m^{-1}.s^{-1}$
w	terminal velocity of a grain in water	$m.s^{-1}$
γ	specific weight of a grain in water	$N.m^{-3}$
τ_0	shear stress exerted by the flow on the bed	$N.m^{-2}$
τ_c	critical shear stress required to initiate sediment movement	$N.m^{-2}$

2.2 INTRODUCTION TO SEDIMENT TRANSPORT

Sediment transport in fluvial environments is a component of the broad discipline of Physical Sedimentology. Physical Sedimentology is about: (1) the interplay that occurs within the Earth's natural environments between solid transportable particles and transporting (or potentially transporting) fluids; and (2) the sedimentary consequences of that interplay (Allen, 1985).

The fluvial environment is an integral part of man's existence. Since the development of early civilizations along rivers such as the Yellow River in China, the Nile River in Egypt and the Tigris-Euphrates in Iraq, until present day, man has relied on rivers for fresh water, irrigation, transportation and as an energy source. A river is characterised by the geology, hydrology, topography, hydraulics and ecology of its drainage basin. The dependence of man on rivers has necessitated the study of the influence of these factors on river systems. Changes in these factors may be either due to natural phenomena or due to human interference.

An example of the effect of changes on a river system can be seen at St Lucia Estuary Mouth. In the last 50 years poor farming techniques have increased erosion in the catchment resulting in increased siltation of the estuary mouth region. This illustrates the consequences of mans' interference: the scouring of the estuary mouth by the September 1987 floods is a good example of the effects of a change due to a natural event.

The histories of hydraulic and sediment engineering are well documented in Simons and Senturk (1976). A brief summary of the major contributions is given here. The earliest records of hydraulic engineering are from about 4000 B.C. when Yu constructed several dikes to protect the fertile plains of China from floods. At about the same time King Menes of Egypt had a dam constructed on the Nile River as part of an irrigation scheme. The first reference to sediment transport is attributed to Hippocrates, 400 BC, who separated sediment particles into size fractions based on settling velocities. The Greek and the Romans were notable hydraulic engineers but neglected to develop sediment transport and river hydrology theory. From this period until the Renaissance progress in these fields was slow and sporadic.

Leonardo Da Vinci (1452-1519) observed sediment movement in flume experiments and related bed material to the type of water motion. Guglielmini (1655-1710) published the first book on sediment engineering "Della Natura de Fiumi", which is based on field observations. During the Eighteenth century several notable advances occurred. Dubuat (1734-1809) wrote "Principé d'Hydraulique". In this he noted: the

velocities necessary to move rock particles of various sizes; the formation and migration of sand waves; and the armouring effects by coarser fractions of the bed load. Chezy (1718-1798) devised the uniform flow formula used to estimate the average flow velocity in an open channel which is dependent on slope, hydraulic radius and a resistance factor which reflects the boundary conditions. This equation is still in wide use today.

The development of sediment transport technology during the eighteenth century was greatly enhanced by the contributions of the following mathematicians and physicists; Bernoulli, Euler, Laplace, Lagrange and Gauss. This trend continued into the nineteenth century when several flow equations were developed by the likes of Navier, Froude, Barre de Saint Venant, Manning, Stokes, Reynolds and Boussinesq.

The first explanation for sediment transportation by suspension was given by Dupuit in 1848, who ascribed this phenomenon to the greater flow velocity above the particle as opposed to below. In 1871 Partiot observed saltation and noted that most sediment is transported as bed load except in areas of great turbulence. Du Boys in 1879 was the first to formulate a sediment transport equation for the bed load. He described a tractive force and determined a critical value for each kind of material based on size. He derived his equation on the assumption that only once the tractive force exceeded the critical value could sediment transport occur. He also stated that the amount of sediment transported was influenced primarily by slope and secondly by flow depth.

Since Du Boys work numerous transport equations for both suspended and bed load sediment have been developed. These equations can be classified by the way in which they were derived. Some of the different types of derivations for bed load transport equations are based on:

(1) excess tractive force, eg. Duboys (1879);
(2) probabilistic theory, eg. Einstein (1942);

(3) empirical data, eg. Meyer-Peter and Muller (1948);

(4) non-fluctuating time averaging techniques, eg. Yalin (1963);

(5) stream energy considerations, eg. Bagnold (1966).

Each of the above types of equation and their inherent assumptions will be discussed. Then, by looking at the properties of St Lucia Estuary Mouth, a recommendation will be made for the selection of a particular bed load sediment transport equation best suited to the study area.

It is important to note that all the sediment transport models were derived for the idealised conditions of steady uniform flow and for cohesionless sediment particles. Recently attempts have been made to model sediment transport for more realistic conditions, for example: "Unsteady Sediment Transport Modelling", by D.A. Lyn (1987); and "Sediment Transport in Oscillatory Flow over Flat Beds", by R.V. Ahilan & J.F.A. Sealth (1987). These models are still in their infancy and thorough testing is still required.

2.3 DU BOYS' EQUATION

2.3.1 Symbols used by Du Boys

C_d	characteristic sediment coefficient	
C_f	a dimensionless frictional coefficient	
d'	thickness of sediment layer	m
Δu	difference of velocity between adjacent sediment layers	$m.s^{-1}$
n	number of layers in motion	

2.3.2 Derivation of Du Boys' Equation

The Du Boys type equation relates the sediment volume transport rate to the excess shear stress, as follows:

$$q_{bv}=A\tau_o(\tau_o-\tau_c) \qquad (2.1)$$

Where A is a coefficient dependent on sediment size. In his derivation Du Boys assumed that when the flow velocity increased to such an extent that the critical shear stress required to initiate sediment movement was exceeded, a carpet of sediment with a thickness of one grain diameter started moving. This movement then induced motion in the layer

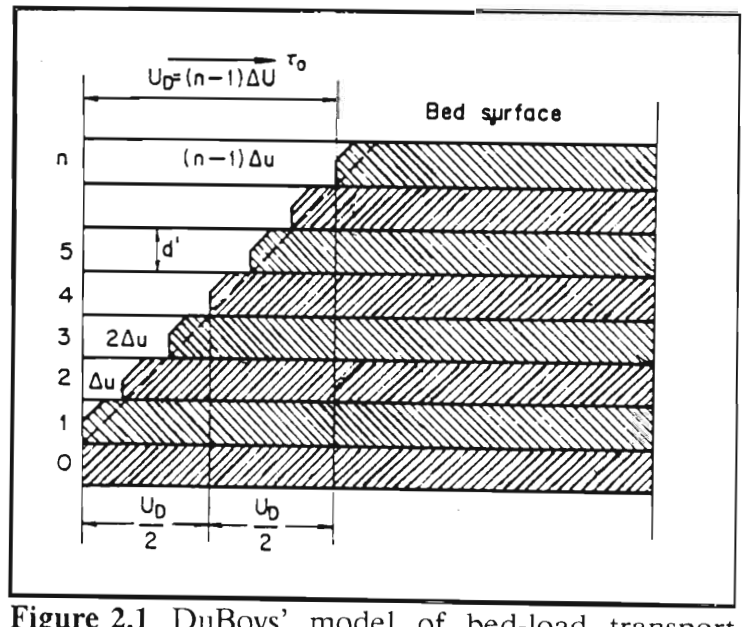

Figure 2.1 DuBoys' model of bed-load transport (DuBoys 1879 in Simons & Senturk, 1976)

of grains directly below it. This process of inducing motion in the layer below continued until the tractive force of the flow was balanced by the frictional force between the successive layers. Du Boys assumed that the layers have the same thickness **d´** and the mean velocity of the successive layers decreased linearly down to the stationary layer. If the velocity decrement between two adjacent layers is given by Δu and the n^{th} layer is stationary, as seen in figure (2.1), then the volume transport rate of the bed load per unit width is given by the product of the average velocity **(n - 1)Δu/2** and the total thickness **nd´**, that is,

$$q_{bv}=\frac{d'\Delta un(n-1)}{2} \tag{2.2}$$

The shear stress exerted by the flow on the bed, τ_0, is balanced by the frictional forces between the successive layers, thus,

$$\tau_o=C_f(\gamma_s-\gamma)nd' \tag{2.3}$$

where $\mathbf{C_f}$ is a dimensionless frictional coefficient.

The critical shear stress required to initiate motion occurs when the top layer is about to start moving or in other words when **n = 1**. Thus,

$$\tau_c=C_f(\gamma_s-\gamma)d' \tag{2.4}$$

or,

$$n=\frac{\tau_o}{\tau_c} \tag{2.5}$$

Substituting this expression back into equation (2.2), gives Du Boys bed load transport equation:

$$q_{bv}=C_d\tau_o(\tau_o-\tau_c) \tag{2.6}$$

Where $\mathbf{C_d}$ is the characteristic sediment coefficient. According to Vanoni (1977), Straub carried out a series of experiments using a small laboratory flume with a sand bed to determine expressions for $\mathbf{C_d}$ and τ_c. In metric units they are as follows,

$$C_d=\frac{0.17}{d^{3/4}} \tag{2.7}$$

$$\tau_c=0.061+0.093d \tag{2.8}$$

Although the concept of critical shear stress has become a fundamental part of sedimentology, the actual mechanical process of sediment transport described by Du Boys has since been shown to be incorrect. According to Yalin (1972), it was Krey in 1910 who first observed that only the grains on the bed surface can be brought into motion by the flow. The 'carpet like' movement has also been shown to be inaccurate. If the shear stress exceeds the critical shear stress the grains advance either in a series of small jumps, this process is known as saltation, or less commonly by rolling. A small proportion of the larger grains may slide. If the shear stress continues to increase further and exceeds a second critical value only a part of the sediment is transported as bed load the remainder is transported in suspension.

2.4 EINSTEIN'S EQUATION

2.4.1 Symbols used by Einstein

A_*	universal constant formed by combining all the α_i's defined in Einsteins derivation, $i \in \{1;b;L;t;w\}$	
B_*	universal constant	
L	saltation length	m
P_n	probability of n saltations in time T	
T	time of grain	s
ζ	hiding factor	
η_0	universal constant	
ϕ	dimensionless sediment transport rate of H. A. Einstein	
Ω	unit area	m^2

2.4.2 Derivation of Einstein's Equation

Einstein used an approach which deviated from the conventional wisdom at the time. He avoided the critical flow criterion for the initiation of sediment movement due to the fact that after interpreting the results of his and several other scientists experiments, no distinct critical value could be established. He also attributed bed load transport to turbulent fluctuations rather than the average values of the forces that the flow exerts on the sediment particles. This second assumption was justified with the following logic: if the sediment transport rate is a function of the average flow velocity alone, then once the flow velocity is increased to such a rate that the first particle starts moving, the force acting on all similar particles will start moving these too. If the bed consists of uniform particles, they would all start moving simultaneously, they would be unable to settle and the sediment transport rate would be determined by the availability of particles only. From experimental evidence this hypothesis is incorrect. He thus approached the problem from a statistical view point

by introducing a probability function which related the instantaneous hydrodynamic lift forces and the particles submerged weight. Using this function his sediment transport equations do not show a sudden discontinuity at the critical shear stress level. In a series of experiments Einstein (1942), noted the following about the relationship between the bed material and the bed load:

(1) a steady exchange between the particles of bed material and the bed load occurs;

(2) particles are transported in a series of steps, the average step length being proportional to the particle size, and do not stay constantly in motion but are deposited after a few steps:

(3) the rate of deposition depends on: (a) the transport rate past a given point; and (b) the probability that the hydrodynamic lift forces are such that the particles may be deposited.

(4) the rate of erosion depends on: (a) the number and properties of the particles; and (b) the probability that the instantaneous hydrodynamic lift forces are large enough to move the particles.

Using the above assumptions Einstein's equations can be derived as follows:

Note that when deriving the equations identical grains are assumed, the procedure may also be used for a mixed bed by replacing the uniform grain characteristics with the average grain characteristics.

Consider an area Ω on the channel bed which is large in comparison to the grain area $\alpha_1 D^2$ and a time interval **T** which is large compared to the average duration of a grain's jump. Let P_n be the probability of a grain having **n** detachments in a time **T**. Each detachment means the grain undergoing an average jump of length **L**. Note that in Einstein's original paper, "Formulas for the Transportation of Bed Load",

(1942) he specified **P**, instead of $\mathbf{P_n}$, where **P** is just the probability of a detachment. The more complex statistical approach of $\mathbf{P_n}$ was presented in his paper, "The Bed Load Function for Sediment Transport in Open Channel Flow", (1950). The later approach will be used here.

From the above the number of grains from an area **Ω**, which are displaced by a distance of at least **nL**, during the time interval **T** can be given as,

$$P_n \frac{\Omega}{\alpha_1 D^2} \tag{2.9}$$

Let **Ω** have unit width and a length equal to an average jump length **L**, that is, **Ω = L.1** ,see figure (2.2).

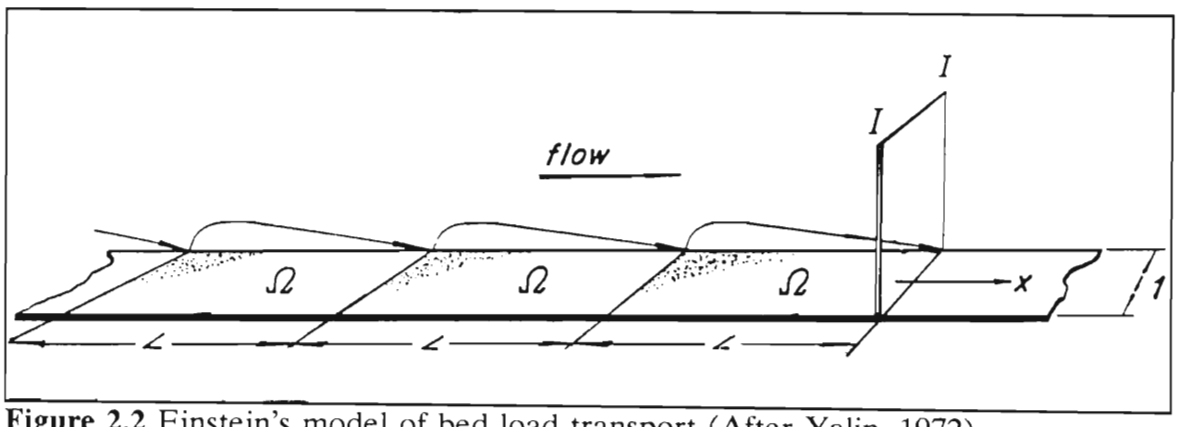

Figure 2.2 Einstein's model of bed load transport (After Yalin, 1972)

The number of grains passing through a point section **I-I** will thus be,

$$\sum_{n=0}^{\infty} P_n \frac{\Omega}{\alpha_1 D^2} = \frac{L}{\alpha_1 D^2} \sum_{n=0}^{\infty} P_n \tag{2.10}$$

Dividing the above expression by **T** gives the number of grains passing through the section per unit time. Then multiplying this by the volume αD^3 of the individual grains gives an expression for the sediment discharge rate by volume at the section **I-I**. This is converted to a sediment discharge rate by weight by multiplying by the specific weight of the grains in water γ_s.

$$q_{bw}=\frac{\alpha_b \gamma_s D}{\alpha_1}\frac{L}{T}\sum_{n=1}^{\infty} P_n \qquad (2.11)$$

As mentioned earlier Einstein assumed that the jump length is proportional to the size of the grain **D**, thus,

$$L=\alpha_L D \qquad (2.12)$$

Another assumption of his was that **T** is proportional to the 'time of the grain', or in other words the time a particle requires to settle, a distance equal to its own diameter, in water. The reason for choosing this time was that it is the only expression with dimensions of time, which is representative for the behaviour of the particle in a liquid, without including any flow characteristiccs. Thus **T** can be expressed as follows,

$$T=\alpha_t \frac{D}{w} \qquad (2.13)$$

The terminal velocity **w** can obtained using the equation for settling velocity derived by Rubey (1933), which is,

$$w=\alpha_w\sqrt{\frac{\gamma_s D}{\rho}} \tag{2.14}$$

where α_L, α_t and α_w are regarded as constants. Combining all the proportionality constants to give A_* and forming the dimensionless sediment discharge rate ϕ equation (2.11) becomes,

$$A_*\phi=\sum_{n=1}^{\infty} P_n \tag{2.15}$$

where A_* and ϕ are as follows,

$$A_*=\frac{\alpha_1\alpha_t}{\alpha\alpha_L\alpha_w} \tag{2.16}$$

$$\phi=\frac{q_{bw}\rho^{1/2}}{(\gamma_s D)^{3/2}} \tag{2.17}$$

Now using probability theory Einstein stated that,

$$\sum_{n=1}^{\infty} P_n=\sum_{n=1}^{\infty} P_1{}^n \tag{2.18}$$

and since $P_1 < 1$, the sum on the right hand side converges to the limit,

$$\sum_{n=1}^{\infty} P_1^{\,n} = \frac{P_1}{1-P_1} \tag{2.19}$$

The events 'at least one detachment' and 'no detachments' are complementary, or in other words $P_1 = 1 - P_0$. The probability of no detachments can be expressed as a function of Ψ. The variable Ψ which is introduced is just the inverse of the sediment mobility number. The sediment mobility number relates the lift forces on a grain to the submerged grain weight. Thus an increase of Ψ implies a greater probability of 'no detachments'. Using this and fitting the probability of 'no detachments' to a normal distribution curve Einstein arrived at his bed load transport equation,

$$1 - \frac{1}{\sqrt{\pi}} \int_{-(B_*\psi + 1/\eta_0)}^{(B_*\psi - 1/\eta_0)} e^{-\xi^2} d\xi = \frac{A_*\phi}{1 + A_*\phi} \tag{2.20}$$

Where Einstein stated that A_*, B_* and η_0 are universal constants, (a statement which was later shown to be incorrect by Yalin (1972)). A derivation of equation (2.20), including expressions of B_*, ξ and η_0, is given in Einstein (1942). In Einstein's (1950) work, he introduced a more sophisticated probability function which allowed for the incorporation of different sediment particle sizes. To do this a factor ς was introduced into the expression of Ψ. The factor ς is known as the hiding factor. This allows for the correction of the lift force which is required when smaller grains 'hide' between the other grains. Obviously for uniform sediment as was used in the above derivation $\varsigma = 1$. Fitting this theory to experimental data Einstein drew up the 'ϕ - Ψ' curve, see figure (2.3).

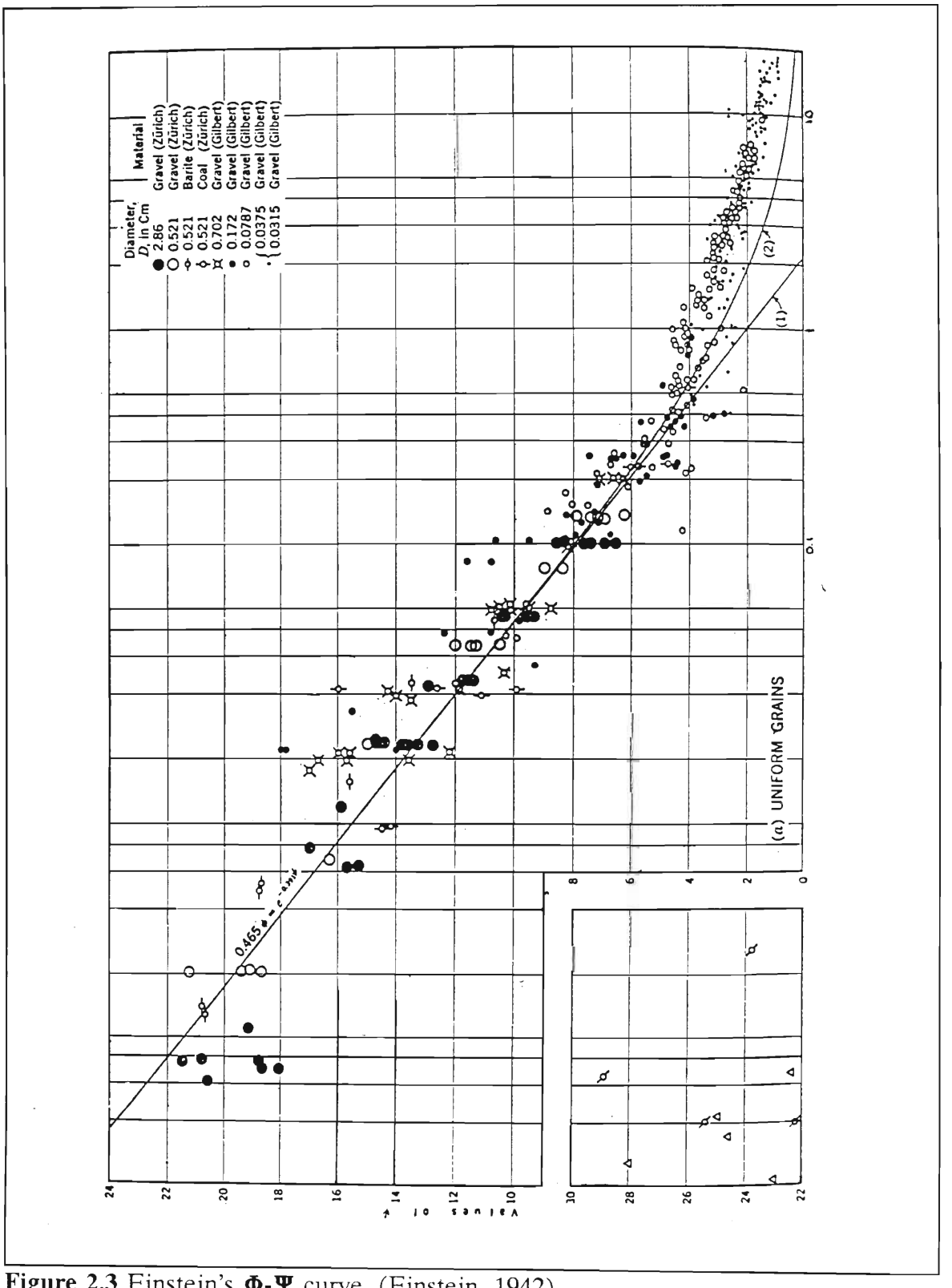

Figure 2.3 Einstein's **Φ-Ψ** curve. (Einstein, 1942)

2.5. MEYER-PETER & MULLER'S EQUATION

2.5.1 Symbols used by Meyer-Peter and Muller

q	flow rate of Meyer-Peter	$lb.ft^{-1}.s^{-1}$
q_b	bed load transport rate of Meyer-Peter	$lb.ft^{-1}.s^{-1}$
S'	part of slope required to overcome the grain resistance	
k'	grain roughness	$m^{1/3}.s^{-1}$

2.5.2 Derivation of Meyer-Peter & Muller's Equation

Meyer-Peter had carried out a series of experiments on well- sorted, coarse grained sediments in flumes with varying width and flow depth. According to the ASCE Task Committee (1971), from the results he developed the empirical formula,

$$q_b^{2/3} = 39.25q^{2/3}S - 9.95D_{50} \qquad (2.21)$$

This equation being valid only for the foot-pound-second system of units. Noting that the coarse sediments used did
not produce rugged bedforms, this equation should only be used in flow where resistance due to bedforms constitutes a small part of the total resistance.

After further experiments with a greater range of sediment type, grain size, flume width and flow depth, a more sophisticated sediment transport equation was put forward by Meyer-Peter & Muller. This equation relates the bedload discharge to the difference between the effective shear and the critical shear. The equation has the improvement of being dimensionally homogeneous thus it is applicable to any consistent set of units.

The equation is adapted to include graded sediments by defining an effective diameter $\mathbf{D_m}$,

$$D_m = \sum_{i=0}^{i=\infty} p_i d_i \qquad \textbf{(2.22)}$$

Where $\mathbf{d_i}$ is the grain diameter for the $\mathbf{i^{th}}$ fraction of the total bed load and constitutes $\mathbf{p_i}$ of the total bed load weight. The sediment transport equation is,

$$\left[\frac{q_b(\gamma_s-\gamma)}{\gamma_s}\right]^{2/3}\left(\frac{\gamma}{g}\right)^{1/3}\frac{0.25}{(\gamma_s-\gamma)D_m} = \frac{(k/k')^{3/2}\gamma\, R\, S}{(\gamma_s-\gamma)D_m} - 0.047 \qquad (2.23)$$

The quantities **k** and **k'** are the reciprocals of the Manning roughness coefficient, that is,

$$U = k\, R^{2/3}\, S^{1/2} \qquad \textbf{(2.24)}$$

$$U = k'\, R^{2/3}\, (S')^{1/2} \qquad \textbf{(2.25)}$$

where **S'** is the part of the total slope, **S**, required to overcome the grain resistance.

k' can be obtained from Strickler's formula for grain roughness,

$$k' = \frac{26}{(D_{90})^{1/6}} \qquad (2.26)$$

D_{90} is the grain size of the bed material for which 90% of the grains are smaller.

The advantage of this later formula over the Meyer-Peter formula is that it can be used for graded sediments which give rise to bed forms. The experiments had no appreciable amounts of suspended sediment and thus the equation should only be used as a bed load formula.

2.6 YALIN'S EQUATION

2.6.1 Symbols used by Yalin

a	function of Z and Y_{cr}	
$C_{x,m}$	the horizontal component of the mean grain velocity during a saltation	$m.s^{-1}$
q_b'	dimensionless sediment transport rate	
s	dimensionless excess shear stress	
W	dimensionless flow depth	
X	grain size Reynolds number	
Y	mobility number	
Z	density ratio of solid and fluid phases	
β	dimensionless flow velocity	
ϵ	sublayer to which grain motion is confined	m
θ_{AC}	dimensionless duration of the grain motion from A to C	
σ	dimensionless distance of the grain motion from A to C	
ψ	inverse of the grain mobility number Y, which is a dimensionless variable	

2.6.2 Derivation of Yalin's Equation

Before proceeding to discuss Yalin's equations the concept of dimensionless variables and the Shields' curve must be introduced. Consider steady, uniform, two-dimensional flow with a free surface of a cohesionless moveable bed. The two-phase motion, or in other words the motion of the fluid and bed material, can be defined by the seven parameters υ, ρ, ρ_s, **D**, **d**, **S** and **g**. **S** and **g** can be substituted with the combinations $\gamma_s = (\rho_s - \rho)\mathbf{g}$ and $v_* = \sqrt{(gSd)}$. Hence any mechanical quantity, eg. q_b or the bed load discharge, of the two-phase motion can be expressed as a function

of the seven characteristic parameters. Since this functional relation q_b is independent of the choice of units of measure, it can be expressed in a dimensionless form q_b' which is a function of the dimensionless variables **W**, **X**, **Y**, and **Z**. These dimensionless variables are,

$$W = \frac{d}{D} \tag{2.27}$$

$$X = \frac{D v_*}{\nu} \tag{2.28}$$

$$Y = \frac{\rho v_*^2}{\gamma_s D} \tag{2.29}$$

$$Z = \frac{\rho}{\rho_s} \tag{2.30}$$

The advantage of this approach is that these four dimensionless variables reflect the influences of the individual parameters **d**, υ, γ_s and ρ_s respectively. The variables **X** and **Y** are more commonly known as the grain-size Reynolds number, which relates the inertial forces of the grain to the viscous forces of the fluid, and the mobility number, which relates the lift forces to the submerged weight of a particle, respectively. In 1936 Shields, according to Yalin (1963), attempted to plot experimental values of Y_{cr} against X_{cr} to produce a curve determining the initiation of sediment movement. The subscript '**cr**' indicating the critical value at which sediment movement commences. He obtained a curve, see figure (2.4), which is still used in engineering applications today.

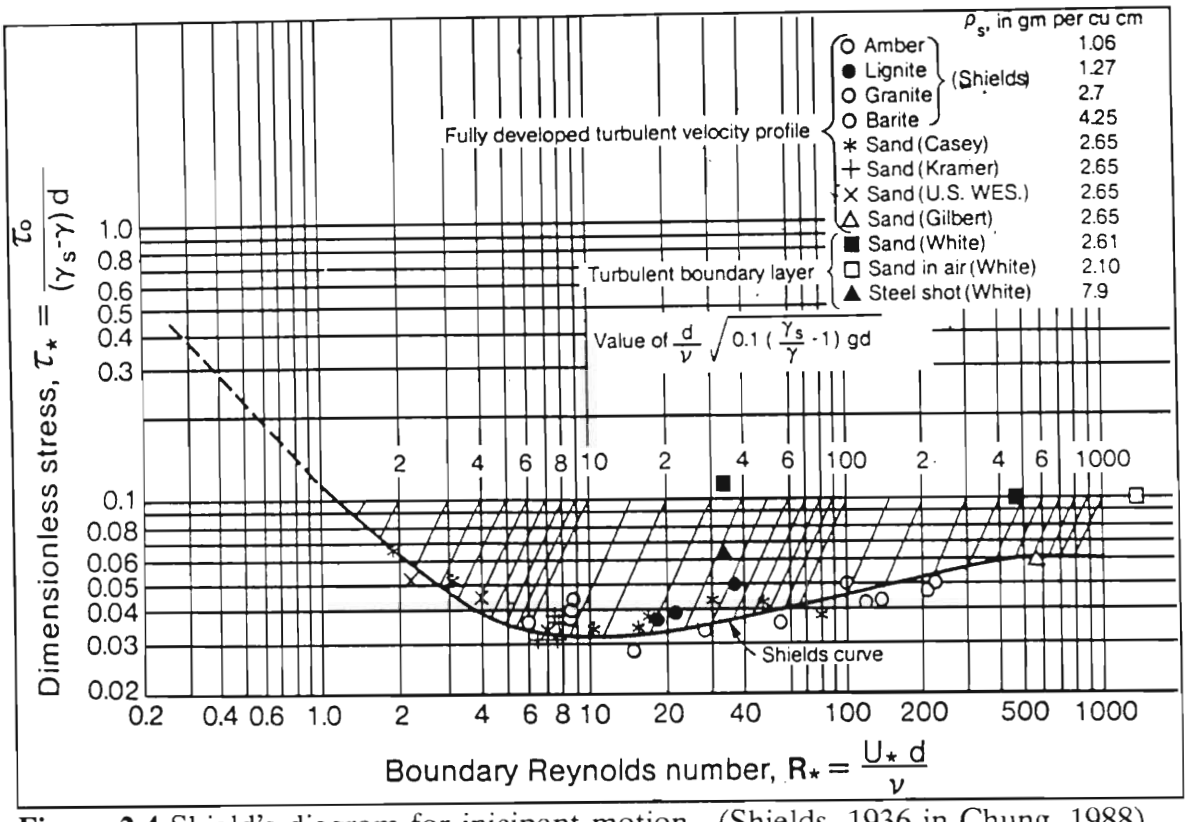

Figure 2.4 Shield's diagram for inicipent motion. (Shields, 1936 in Chung, 1988)

Yalin derived a bed load transport equation for steady, uniform flow of a viscous fluid over a cohesionless moveable bed with uniform sediment particles. He assumed the flow to be turbulent with a laminar sublayer having a thickness less than the bed roughness. He also assumed that the particles are brought into motion once the tractive forces exerted on the particle exceed a critical value, and that when in motion the particles advance by saltation.

Yalin (1963), noted that although Einstein's bed load transport equation correlated well to experimental results in the range $0 < \phi < 1$, it deviated from the experimental points for $\phi > 1$. Yalin attributed this downfall in the equation to the assumptions made by Einstein. Firstly, Yalin stated that the omission of a critical tractive force disregarded the whole concept of the Shields' curve. The Shields' curve indicates experimentally that a critical tractive force exists and also shows how it responds to changes in the grain-size Reynolds number. Secondly, Yalin accepted that the lift forces experienced by individual grains are unequal. However, he attributed this inequality to the sediment particle arrangement as opposed to turbulent fluctuations

suggested by Einstein. Yalin shows this in figure (2.5), where it can be seen if all of the sediment grains are organised in a geometrically perfect sense, the lift forces exerted on each grain would be identical, but this perfection is unrealistic in nature.

Yalin (1963) claimed that Einstein's assumptions are, in a sense, contradictory. He noted: (i) that flow passes through a laminar range prior to becoming turbulent; (ii) that if the critical tractive force does not exist, grain motion can begin immediately after zero velocity. Yalin said that the source of sufficient lift force can not be turbulent fluctuation. On the contrary, if grains are lifted because of turbulent fluctuation, then grain movement cannot begin with the start of flow.

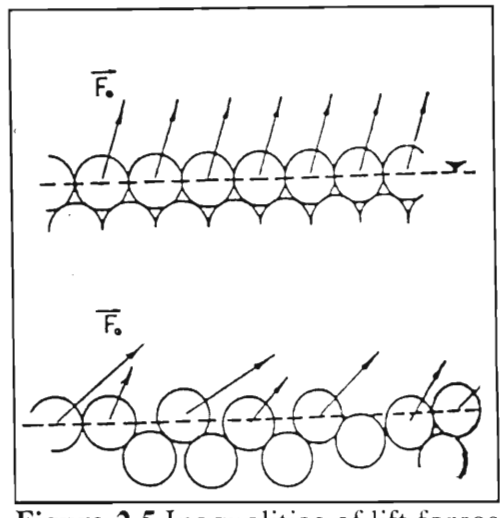

Figure 2.5 Inequalities of lift forces due to imperfect packing. (Yalin, 1972)

Although Yalin raises and criticises these relevant points Einstein's work still has merit for two reasons. Firstly, Einstein fits the probability of no detachments to a normal distribution curve, thus the mean value of Ψ can be interpreted as a 'critical' value of Ψ at which sediment movement is likely to commence. The reason for no sharp discontinuity at this point is that for the values of Ψ greater than the mean, that is where no motion is likely to occur, turbulence may cause variations in Ψ which decrease the local value of Ψ to the mean or 'critical' value. Similarly, for values of Ψ less than the mean, a turbulent fluctuation might increase the value of Ψ to the mean value, thus increasing the likelihood of sediment movement. Thus Einstein is not stating that grains begin moving with the commencement of flow. He is implying that in turbulent flow the mean flow velocity may be a lot less than the critical velocity but turbulent fluctuation may cause local flow to be greater than the critical flow.

Secondly, Yalin assumes turbulent flow having a laminar sublayer with a thickness less than the bed roughness. Grains will therefore protrude into the turbulent layer and will be exposed to fluctuations resulting from turbulence. Thus his assumption that inequalities in lift forces are only due to grain organisation is incorrect. The complete picture for varying lift forces would thus be best described by turbulent fluctuation, uneven grain organisation and other factors not discussed here, for example, the macro bed topography.

Yalin derived his equations from the dimensionless variable approach. He broke down the motion into two stages, namely, the initiation of motion and the dynamics of the saltation, then determined which variables influenced each stage. He assumed that the bed material consisted of uniform grains but due to accepting that the lift forces are unequal he could not assume an identical saltation for all the grains. To overcome this complication he used an 'average' lift force resulting in an 'average' saltation. His derivation can thus be described as a non-fluctuating time-averaging technique. The full derivation will not be given here but the underlying principles will be explained.

As stated earlier q_b' can be described by the variables **W**, **X**, **Y** and **Z**. At the bed the shear stress, $\tau_o = \rho v_*^2$, does not vary with **H**, however the shear stress distribution, τ, is affected by **H**. If the grain motion is confined to a small sublayer, ϵ, so that ϵ/H approaches **0**, then τ can be assumed to be constant. Using this approximation, the influence of **H** and thus **W** no longer affects q_b'. Sediment transport can only commence once the lift force at the bed, L_0, exceeds the grain's submerged weight, **G**. The number of grains in motion, **N**, is thus a function of L_0 and **G**. Since **N** is dimensionless the above function must be in the form of the ratio of the two forces, that is, L_0/G. This ratio can be equated to the ratio Y/Y_{cr}, and sediment movement only occurs when $Y/Y_{cr} > 1$. Therefore **N** is in fact a function of $s = Y/Y_{cr} - 1$. Assuming that the number of grains lifted is directly proportional to the excess tractive force, $N = \text{constant}\ s$. From the Shields' curve Y_{cr} can be related to X_{cr}. Thus the initiation of sediment motion varies with changes in **X** and **Y**.

According to Bagnold (1960), the initial direction of a grain in motion is 'upwards', (figure (2.6)), with a driving force of $\mathbf{L_0}$ - **G** - $\mathbf{R_y}$, where $\mathbf{R_y}$ is the resistance of the fluid. During this upward motion in the region **OA** the grain receives its 'initial' velocity for the remainder of the saltation described by **ABC**. Expressing the grain motion as a differential equation and solving, gives the initial velocity.

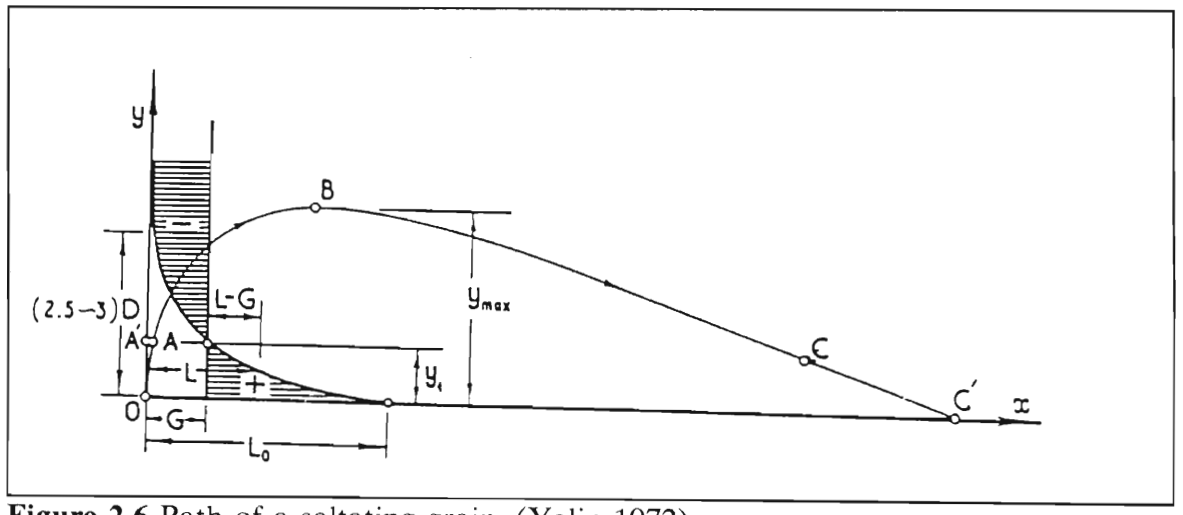

Figure 2.6 Path of a saltating grain. (Yalin,1972)

In nature, the whole saltation of a grain occurs within the turbulent layer, therefore the effect of υ and thus **X** can be
neglected during the saltation. Bearing this in mind the equations of a particle in motion for both the **x** and **y** directions can be set up with the previously obtained velocity being used as an initial condition. From these the duration, height and mean horizontal velocity, $\mathbf{C_{x,m}}$, of the saltation can be determined.

The expression for $\mathbf{C_{x,m}}$ is given as,

$$C_{x,m}=v_* \beta[1-\frac{1}{\sigma}\log(1+\sigma)] \qquad (2.31)$$

where $\boldsymbol{\beta} = \mathbf{10}$ and $\boldsymbol{\sigma} = \boldsymbol{\beta\theta_{AC}}$ which is the dimensionless expression of the distance taken for a grain to move from **A** to **C**.

The value of q_b' is given by product of the number of grains in motion and the mean horizontal velocity of the grains,

$$\frac{q_b}{\gamma_s D v_*} = q_b' = NC_{x,m} = constant\ s\left[1 - \frac{1}{\sigma}\log(1+\sigma)\right] \qquad (2.32)$$

From experiments $\sigma = as$ where **a** is a function of **Z** and Y_{cr}, and **s** is the dimensionless excess of the shear stress. Thus Yalin's sediment transport equation can be expressed as,

$$q_b' = constant\ s\left[1 - \frac{1}{as}\log(1+as)\right] \qquad (2.33)$$

where the value of the constant can only be determined experimentally. Using the same data as that used by Einstein, Yalin obtained the value for the constant and converting his q_b' function into the Ψ function of Einstein's compared the two sets of results, see figure (2.7). Yalin's equation can be seen as a family of curves orresponding to different grain diameters.

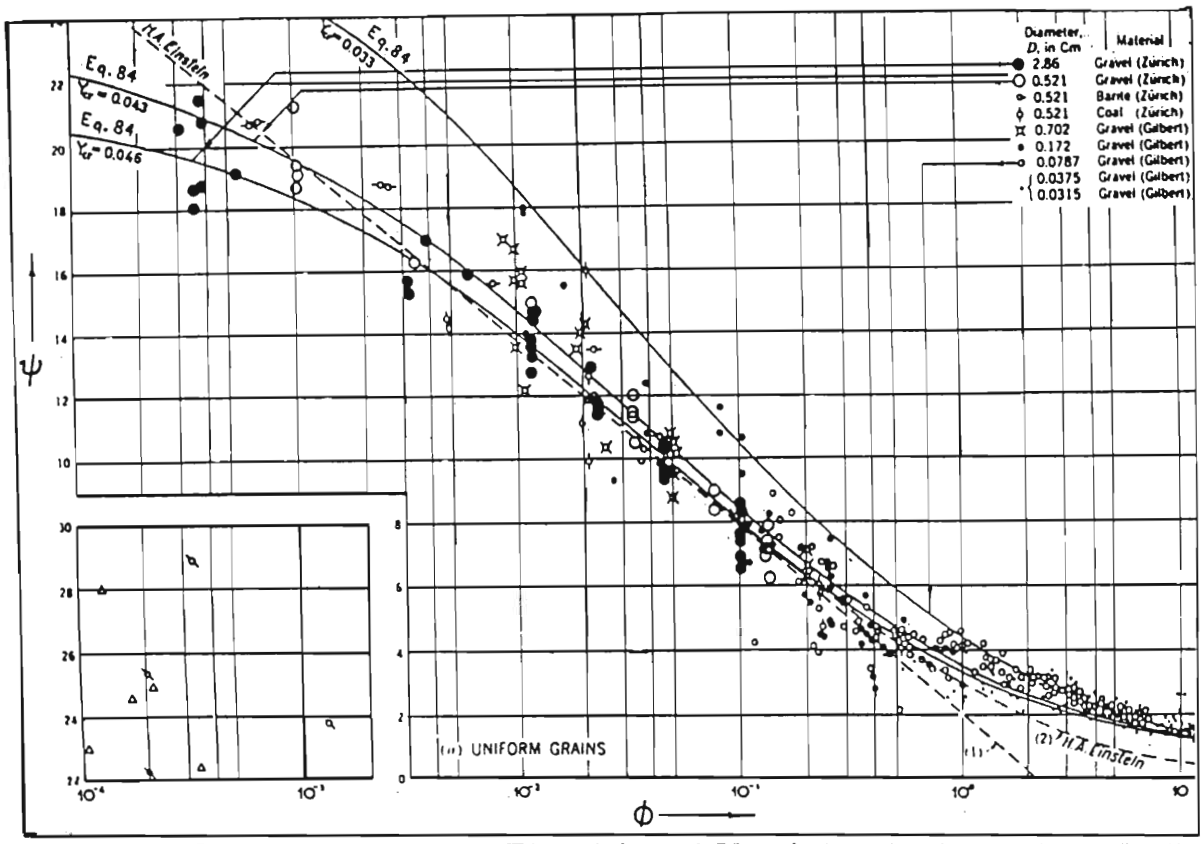

Figure 2.7 Comparision between Einstein's and Yalin's bed load equations. (Yalin 1963)

2.7 BAGNOLD'S EQUATION

2.7.1 Symbols used by Bagnold

e	transport efficiency	
i	transport rate of solids by immersed weight per unit width	$N.s^{-1}$
m	mass of transported solids over unit bed area	kg
P	stress transmitted from solid to solid normal to the shear plane	N
T	stress transmitted from solid to solid tangential to the shear plane	N
U	mean flow velocity	$m.s^{-1}$
V	fall velocity of suspended solids	$m.s^{-1}$
$\tan\alpha$	coefficient of solid friction	
θ	dimensionless shear stress	
σ	density of solids	$kg.m^{-3}$
τ	mean boundary shear stress	N
Ω	stream power per unit length of whole stream	$W.m^{-1}$
ω	stream power per unit boundary area	$W.m^{-1}$

Subscipts

b	bed load
s	suspended load

2.7.2 Derivation of Bagnold's Equation

Bagnold originally derived a bed load sediment transport formula based on energy principles (1956). Bagnold enhanced this idea and in 1966 he published his paper " An Approach to the Sediment Transport Problem from General Physics" (Bagnold,

1966) in which he derived a total load sediment transport formula. Until now only the bed load formulae of several authors have been discussed, however Bagnold's total load equations will be examined as in his 1966 paper Bagnold simplified and modified his original tentative conclusions.

Bagnold's total load expression relates the sediment transport rate to the expenditure of power by the fluid flow. According to Bagnold (1966) previous sediment transport studies tended to avoid energy considerations due to the obvious difficulty in predicting precise energy states at any point within the flow. To avoid this problem, Bagnold used a statistically steady flow; or in other words, a flow which is representative of the average flow along a channel reach taking into consideration irregularities in physical boundary conditions and consequent fluctuations in energy states. Other specifications required for the total load formula to hold are: (i) that there is an unlimited availability of transportable solids; and (ii) that the concentration of solids in the liquid is such that the gravitational pull on the solids has no appreciable effect on the tractive stress of the fluid.

Approaching sediment transport from the principles of general physics the following factors need to be identified:

1. the type of motion;
2. how the motion is maintained;
3. how the magnitude of the maintaining forces and the sediment transport rate are related.

Bagnold claimed that sediment transport is a two phase flow with successive layers of sediment shearing over each other. This is much the same as the Du Boys-type carpet movement. For a solid to shear it must undergo some dispersion (Reynolds, 1885) and thus an upward supporting stress is required below a shear plane. For steady motion the upward supporting stress at any point must equal the immersed weight of the solids above it. Bagnold stated that the upward supporting stress is generated by momentum transfer either from solid to solid or from fluid to

unsupported solid. He later used these two mechanisms to distinguish between bed load (solid to solid) and suspended load (fluid to solid) sediment transport. The maintenance of the upward supporting stress is attributed by Bagnold to the tractive force of the fluid. Bagnold relied on the power equation to relate the magnitude of the forces to the sediment transport rate,

$$\text{rate of work} = \text{available power} \times \text{efficiency} \qquad (2.34)$$

The available power of a liquid per unit of channel length, **Ω**, is the amount of kinetic energy that is liberated as it descends a slope, **S**.

$$\Omega = \rho g Q S \qquad (2.35)$$

Thus the mean available power supply to the column of fluid over bed area, **ω**, is therefore

$$\omega = \frac{\Omega}{flow\ width} = \rho g d S U = \tau U \qquad (2.36)$$

where **U** is the mean flow velocity and **τ** the mean boundary shear stress.

Bagnold calculated the work rate as two components; the separate work rates associated with transporting the bed load and suspended load sediments independently. Using principles of solid friction, he derived the equation for the bed load work rate as the product of the transport rate of the immersed sediment ,$\mathbf{i_b}$, and the coefficient of dynamic friction, **T/P**.

Where $\mathbf{i_b}$ is

$$i_b = \frac{\sigma - \rho}{\sigma} m_b g U_b \qquad (2.37)$$

and **T/P** is the ratio of the tangential shear stress required to initiate sediment motion and the normal pressure. According to Bagnold (1956) the coefficient of dynamic friction is of the same order as the coefficient of static friction, the latter being easily measurable as $\tan\alpha$, where α is the angle of repose at which shearing commences. Thus, using $\mathbf{e_b}$ as the efficiency associated with bed load work rate, equation (2.34) becomes

$$i_b = \frac{\omega e_b}{\tan\alpha} \qquad (2.38)$$

When deriving the expression for the suspended load work rate Bagnold used the logic that, although the sediment in suspension is falling with a mean velocity of **V** relative to the fluid, the centre of mass of the sediment remains in suspension. From this he deduced that the fluid must be lifting the sediments with the equivalent velocity **V**. Noting that i_s is defined as

$$i_s = \frac{\sigma - \rho}{\sigma} m_s g U_s \qquad (2.39)$$

and that after bed load transport the available power left for suspended load transport is $\omega(1 - e_b)$, equation (2.34) for suspended load becomes

$$i_s = \omega(1 - e_b) e_s \frac{U}{V} \qquad (2.40)$$

From equations (2.38) and (2.40) Bagnold gave a total transport rate for the immersed sediment weight, **i**, where,

$$i = i_b + i_s = \omega\left(\frac{e_b}{\tan\alpha} + \frac{e_s U_s}{V}(1 - e_b)\right) \qquad (2.41)$$

In the above equation $\mathbf{e_b}$, $\mathbf{e_s}$, $\mathbf{\tan\alpha}$ and $\mathbf{U_s}$ must be specified. Bagnold assumed that $\mathbf{U_s}$ is equivalent **U**, thus he had only to determine values for the remaining three parameters.

To obtain a range of values for $\mathbf{e_b}$, Bagnold looked at the work done by the fluid on the flow boundary. The flow boundary being a zone of finite thickness, at or within which the shear stress of the fluid is reduced to zero by transfer to another medium. A flow boundary might be in motion relative to the ground. Bagnold noted that if the fluid shear stress is sufficiently large, the bed load increases to such an extent that it becomes a moving carpet which occludes the stationary bed from the fluid. If this carpet or boundary layer is moving with velocity U_c, the flow velocity relative to the boundary is $\mathbf{U - U_c}$. Two further observations were also made namely:

(1) that the flow law may be written as

$$\tau = const\,(U - U_c)^n \qquad (2.42)$$

where **n** ranges from 1 for laminar flow to 2 for turbulent flow;

(2) that when the thickness of the flow boundary is negligible in comparison to the flow depth

$$\tau = T \tag{2.43}$$

where **T** is the solid transmitted shear stress.

From the above, the work done in transporting the flow boundary is

$$TU_c = \tau U_c = const\, U_c(U - U_c)^n \tag{2.44}$$

This expression has a maximum value when $\mathbf{U_c = (1 + n)^{-n}}$, thus the maximum efficiency with which the boundary may be transported, $\mathbf{e_c}$, is

$$e_c = \frac{TU_c}{\tau U} = \frac{1}{1+n} \tag{2.45}$$

Thus $\mathbf{e_c = 1/3}$ for fully turbulent flow.

Dispersed solids do not behave as a continuous carpet as individual grains move relative to each other, thus a further efficiency factor, $\mathbf{e_g}$, is required so that

$$e_b = e_c \times e_g \tag{2.46}$$

To obtain $\mathbf{e_g}$ Bagnold used similar reasoning as above resulting in an expression

$$e_g = \frac{1}{n' + 1} \tag{2.47}$$

where **n'** is found from the relationship between the drag coefficient and the Reynolds

number of the grain. (See figure (2.8) for values of e_b and e_g.)

The total energy expended transporting the bed load is thus e_b' plus the ineffective power dissipation $e_c\omega(1 - e_g)$ involved in local transfer of stress from fluid to solid. Summing these two, the stream power utilised is $e_c\omega$ but $e_c = 1/3$, thus 2/3 of the initial available stream power remains for the transportation of a suspended load.

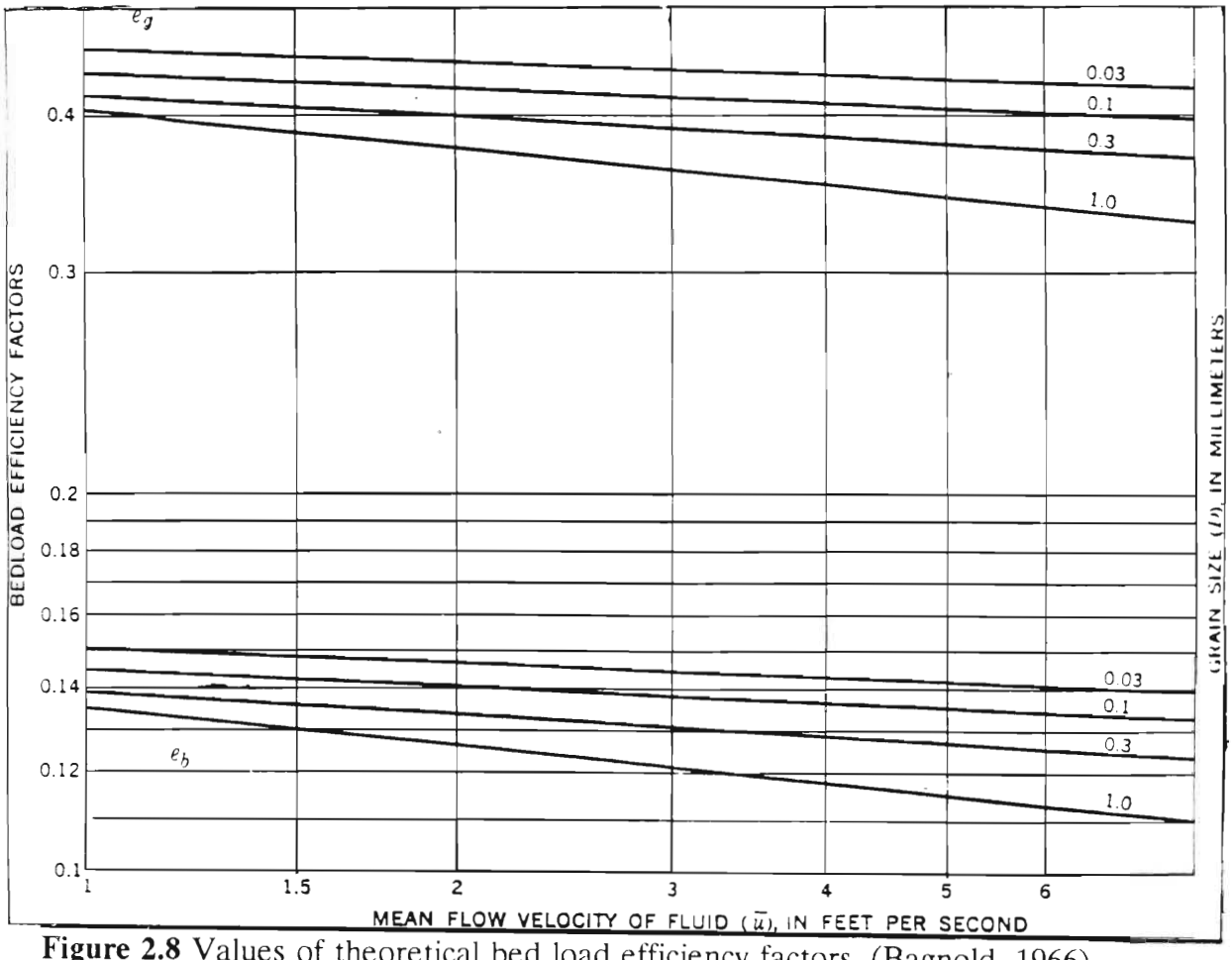

Figure 2.8 Values of theoretical bed load efficiency factors. (Bagnold, 1966)

Bagnold noted that **tanα**, and thus the dynamic bed load friction coefficient, vary by a factor of two depending on the effects of the grain's inertia and the fluid viscosity on the grain motion. The change from viscous to inertial conditions of motion of a grain are related to its diameter and thus the Reynolds number,

$$Re = \frac{D}{\nu}\sqrt{\frac{\tau}{\rho}} \qquad (2.48)$$

provided that the flow is at high stages so that $\mathbf{T} = \boldsymbol{\tau}$, and that the linear spatial concentration of the grains is such that the grains behave as a fluid and not as a 'paste'. Using this relationship and introducing the dimensionless bed shear stress, $\boldsymbol{\theta}$,

$$\theta = \frac{\tau}{(\sigma - \rho)D} \qquad (2.49)$$

Bagnold obtained a family of curves relating $\tan\boldsymbol{\alpha}$ to $\boldsymbol{\theta}$ for quartz-density solids of various sizes in water (figure (2.9)). The critical values of $\boldsymbol{\theta}$, $\boldsymbol{\theta}_x$, being merely the values of $\boldsymbol{\theta}$, and thus $\boldsymbol{\tau}$, beyond which the theory becomes applicable.

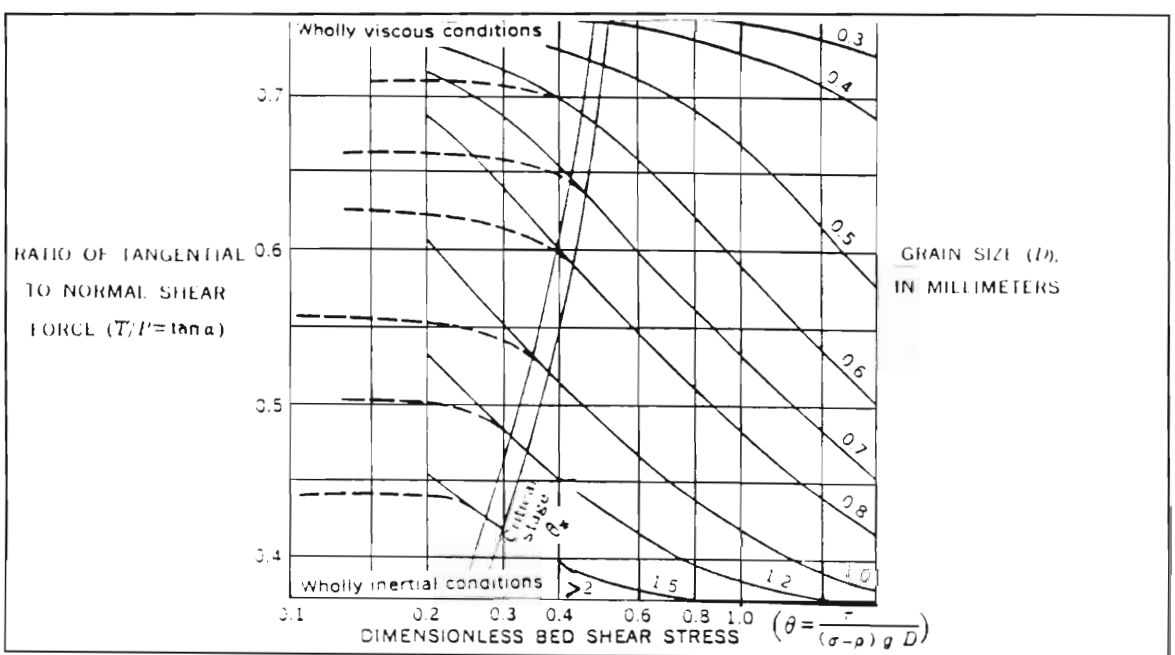

Figure 2.9 Values of the solid friction coefficient tanα in terms of the bed-stress criterion. (Bagnold, 1966)

Finally, to determine the suspended load transport efficiency $\mathbf{e_s}$, it must be noted that isotropic turbulence is incapable of maintaining an upward directed stress to support

a suspended load. This is a consequence of the fact that in isotropic conditions the net upward flux of eddy momentum is equal to the net downward flux, thus any grains will fall through the fluid under the influence of gravity. According to Bagnold (1966), in 1952, Prandtl showed that the fluid motion, relative to the shear boundary, which is induced by turbulence is highly asymmetrical. As can be seen from figure (2.10), there is an initial upward pull of a mass into the upper faster moving layers. The crest of this mass is 'torn' off and the remaining mass gradually sinks back. Obviously no net normal transport can occur, thus for the rapid upwelling to balance the gradual sinking, the upward velocity must exceed the downward velocity of the return flow. Based on Prandtl's observations and work done by Laufer (1954) and Townsend (1956), which related the momentum flux propagation to the shear velocity, Bagnold obtained a constant value for $\mathbf{e}_s$ in fully developed turbulent flow

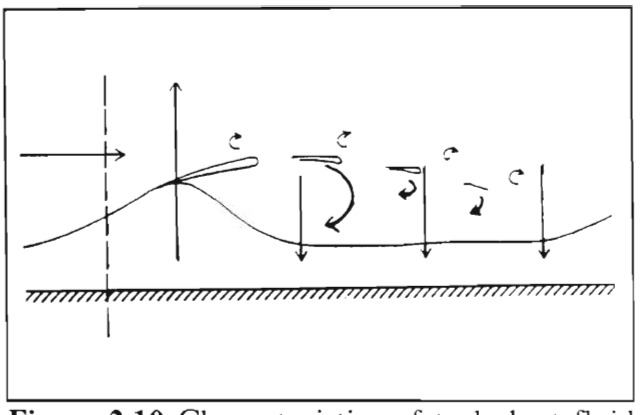

Figure 2.10 Characteristics of turbulent fluid motion. (Prandtl, 1952 in Bagnold, 1966)

$$e_s = 0.015 \tag{2.50}$$

Thus returning to equation (2.41), the total transport rate for the immersed sediment weight becomes

$$i = \omega\left(\frac{e_b}{\tan\alpha} + \frac{0.01\,U}{V}\right) \tag{2.51}$$

Where the coefficient 0.01 is the product of $\mathbf{e}_s$ and the available stream power remaining for the transportation of a suspended load, namely two-thirds of the original power.

2.8 SUITABILITY OF MODELS FOR ST LUCIA

All the sediment transport models discussed were derived for idealised conditions thus none would be able to give an exact mathematical formulation for sediment movements within the St. Lucia Estuary Mouth. Du Boys' model was included in the discussion mainly for historical purposes, as his carpet type motion has been shown to be incorrect. The statistical approach of Einstein has merit, but the data requirements to adapt and utilise such a model would be too large and time-consuming to be a practical proposition. Similarly, the Meyer-Peter and Muller formula, which was obtained empirically for gravitational flow, would have to be altered to tidal conditions, again requiring vast amounts of data.

Finally we are left with Yalin's formula, which looks at individual grain motion, and Bagnold's formula based on stream energy principles. The importance of fluid velocity and the fluid shear stress is common to the models. Both authors make two assumptions: (i) the zone in which bed load transport occurs is negligible compared to the flow depth; and (ii) the flow conditions for which the formulae hold occur when the bedform features (sedimentary structures) vanish. These assumptions do not hold for St Lucia Estuary Mouth due to the existence of large tidal flats, eg. Shark Basin, and different kinds of sedimentary structure ranging in size from flood tidal deltas to small ripple sets. Bagnold also specifies the available energy as a function of the slope, in the St Lucia Estuary Mouth the available energy is also a result of tidal fluctuations. Despite this added complication Bagnold's ideas are probably more suitable than Yalin's. Yalin's model was derived for microscale sediment movements, thus when trying to extrapolate to a scale where the physical properties of both the fluid and solids are continually changing, several problems will be encountered.

From the above it is clearly seen that the first step toward a mathematical model of the sediment movements within the St Lucia Estuary Mouth, would be a hydrodynamic model giving flow velocities at all locations within the channel.

The second step would be to approach the sediment movement problem from stream

energy principles, although a new method, which incorporates tidal fluctuations when determining the available stream power available for the transportation of solids, must be derived. Tidal fluctuations will cause a waxing and waning effect on the stream energy. During flood tides the normal river flow will be opposed by the tidal influx thus reducing both the flow velocity and thus the available stream energy. The opposite occurs during the ebb tide when the tidal flow is in the same direction as the normal river flow, thus the flow velocity and available stream power will be increased. Moreover, when looking at sediment transport in estuarine systems, flocculation of suspended sediment must be considered. According to Swart (1987), 88% of the total sediment load of a river in flood is suspended sediment. When suspended sediment comes into contact with saline water a reaction occurs which causes the grains to accrete, often to such an extent that they can no longer be carried in suspension. The rate at which the suspended load becomes bed load obviously will effect sediment transport rates.

To successfully carry out both these steps a substantial amount of data, regarding flow velocities, under different tidal and lake level conditions, and sediment movements, will have to be collected. In this thesis only the hydrodynamic model will be developed and this using only hypothetical data. In the next chapter one-dimensional models that have been applied to the St Lucia estuary will be reviewed in order to see whether they are suitable to link to a sediment transport model.

CHAPTER 3

ONE-DIMENSIONAL HYDRODYNAMIC MODELS

3.1 NOTATION

a	cross-sectional area of flow region	m^2
A	total cross-sectional area	m^2
b	flow region breadth	m
B	total channel breadth	m
C	Chezy's friction coefficient	$m^{1/2}.s^{-1}$
f	acceleration	$m.s^{-2}$
g	gravitational acceleration	$m.s^{-2}$
H	hydraulic depth (A/B)	m
j	storage region inflow momentum factor	
k	contraction or headloss coefficient	
m	mass	kg
P	wetted perimeter of channel	m
q	rate of lateral inflow of water	$m^3.s^{-1}$
Q	discharge in y-direction	$m^3.s^{-1}$
R	hydraulic radius (A/P)	m
t	time	s
U	flow velocity in the y-direction	$m.s^{-1}$
W	wind shear	N
y	flow axis	m
z	water level	m
α	energy correction factor	
β	momentum correction factor	
$\phi(h)$	frictional function dependant on h	
γ	specific weight of water	$N.m^{-3}$

3.2 HISTORY OF THE ST LUCIA ESTUARY MOUTH

An estuary is the part of a river effected by tides. Applying this definition to the St Lucia System, the estuarine part of the system constitutes the region stretching from the estuary mouth to a point 16 km upstream, called the Forks (James & Horne, 1969: figure (3.1)). To develop a hydrodynamic model for the entire estuary would require a computer with a large memory region due to the necessary number of grid points (this is discussed later in Chapter 5). Thus for this thesis a hypothetical estuary based on the data available for the region extending from the 400 metres inland of the estuary mouth to Honeymoon Bend, which is 2 kilometres inland, is modelled. At a later stage the model could be expanded to incorporate the whole estuary.

St Lucia Estuary provides a vital link between the main St Lucia Lake and the sea (figure 3.2). In the first half of this century poor farming techniques in the Mfolozi River catchment caused increased siltation of the Mfolozi-St Lucia mouth. The Mfolozi River was diverted to a separate mouth in an attempt to relieve the problem. The consequences of this interference were:

(1) to reduce the freshwater input into the main lake system;

(2) to reduce the hydraulic head of St Lucia estuary, thus decreasing its ability to scour the shoals within the mouth.

The unique ecosystem in the lake was adversely affected by the resultant increase in salinity. At this stage a series of hydrodynamic studies on the St Lucia Lake System were initiated.

This chapter discusses the suitability of linking a sediment transport model to some of the mathematical hydrodynamic models which were previously applied to the estuarine region of the St Lucia Lake System. This will be achieved by:

(1) comparing existing mathematical hydrodynamic models which have been applied to the study area;

(2) discussing the requirements for a sediment transport model;

(3) investigating if any of the models satisfy these requirements.

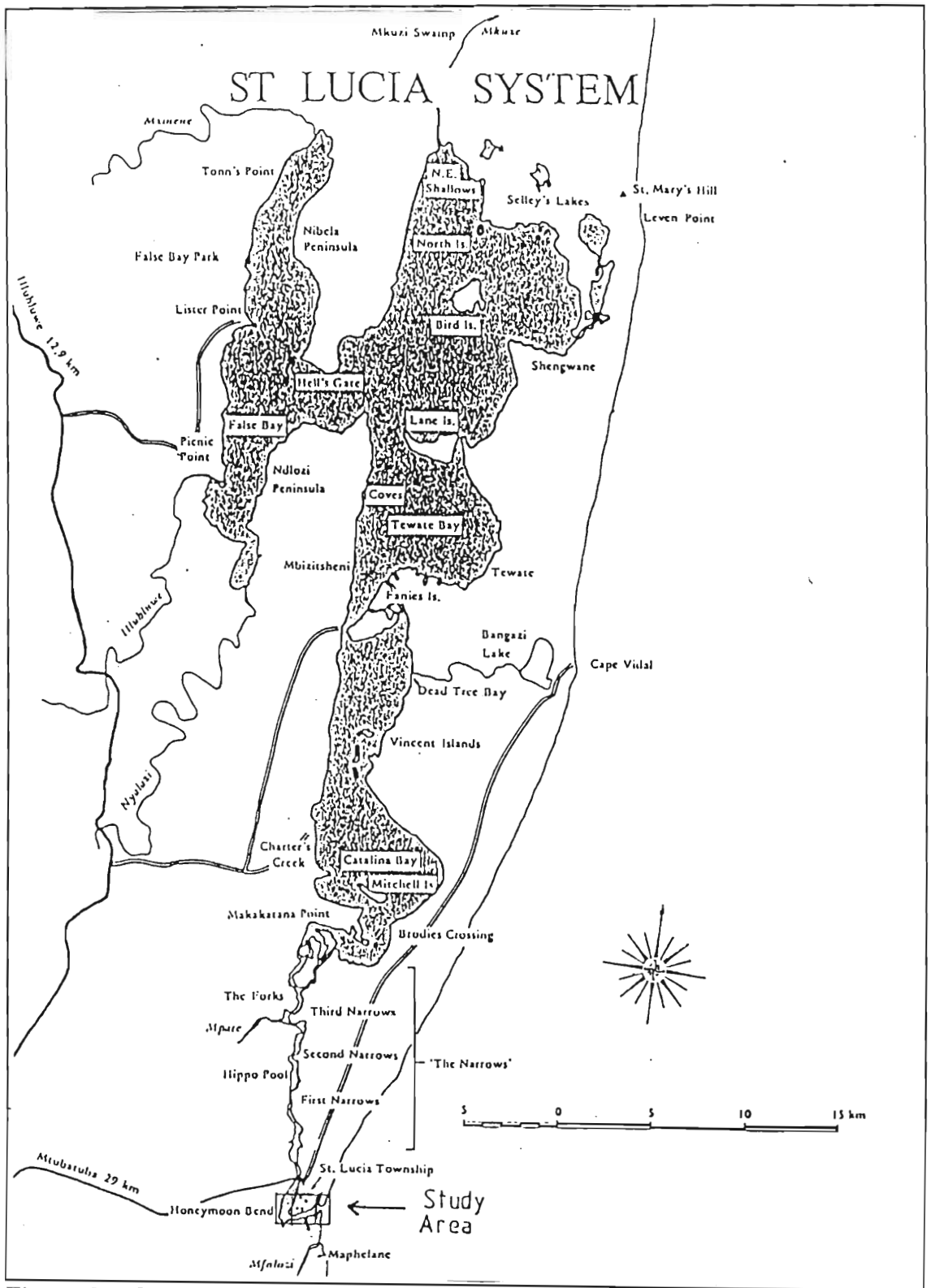

Figure 3.1 Geography of the St Lucia System. (Begg 1978 in Wright 1990)

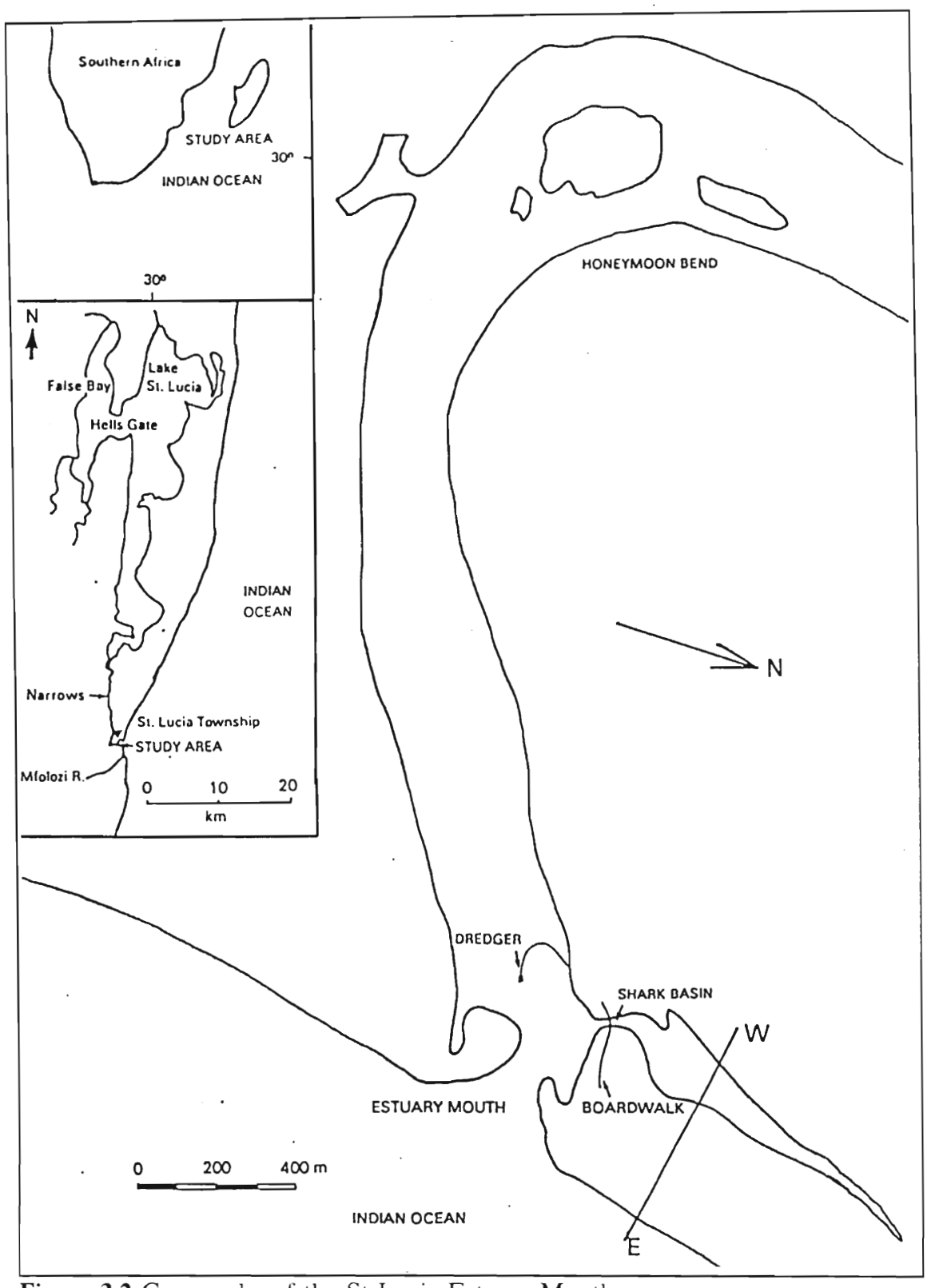

Figure 3.2 Geography of the St Lucia Estuary Mouth (After Wright 1990)

3.3 REVIEW OF ONE-DIMENSIONAL HYDRODYNAMIC MODELS

Several hydrological models have been applied to the St Lucia Estuary. The models can be classified into two groups:

(1) physical models, eg. Sauermann (1966);
(2) mathematical models.

The mathematical models are of concern in this thesis. Three of the most used models were developed by James & Horne (1969), Hutchison (1976) and Huizinga (1987). Hereafter these will be referred to as models 1, 2 and 3 respectively. All three models solve the one-dimensional unsteady (flow varies with time), nonuniform (flow varies with distance along the flow axis), flow equations. These are classified as mass continuity and momentum equations. Model 2 uses the energy equation for reaches where significant changes in channel cross-sectional area occur, such as occurs at the estuary mouth. This is due to the fact that within the proximity of a severe constriction the momentum equation does not deal adequately with the Bernoulli effect. The Bernoulli effect is experienced when an object is subjected to lift forces caused by an imbalance of pressure above and below it: the forces originate from high speed fluid flow around the object. To compare the models the three equations will be written in full, and then, referring to each model, terms which have been neglected will be noted. The method of solution will then be discussed.

3.3.1 Continuity

In order for continuity requirements to be satisfied in a given channel section for a specified time period, the average rates of water outflow and storage area increase must be equal to the average rate of water inflow.
This is expressed by the following equation:

$$\frac{\partial Q}{\partial x} + B\frac{\partial z}{\partial t} = \frac{q}{\delta x} \qquad (3.1)$$

Models 1 and 3 assume that the lateral inflow is negligible, thus the last term in the above equation is zero. James and Horne (1969) justify this assumption from the observation, noted by Natal University Civil Engineering students, under James' supervision (1968), that an abrupt change in flow direction occurs immediately after slack water. If it is not a mixed estuary, or alternatively, if it is an estuary where the fresh river water flows over a tapering salt wedge, exchange flow would have been observed (Leeder, 1982). From this result they assume that the salinity and density in the estuary is constant and thus lateral inflow of freshwater must be negligible.

3.3.2 Momentum

The momentum equation is derived from Newton's Second Law which states that the sum of the forces acting on a body is equal to the product of the mass, **m**, and acceleration, **f**, of the body. The dominant forces applicable to this problem are as follows :

$$F_p + F_g + F_f + F_s + F_q + F_w + F_o = mf \qquad (3.2)$$

F_p = Force due to pressure (N)
F_g = Force due to gravity (N)
F_f = Force due to boundary friction (N)
F_s = Force due to water entering from storage region (N)
F_q = Force due to lateral inflow (N)
F_w = Force due to wind shear (N)
F_o = Force due to obstructions to flow (N)

The Coriolis force is neglected from the above equation as St Lucia Estuary's dimensions and latitude cause it to have negligible effect, see section 4.3.1.

The above equation is expressed as follows in the various models:

Model 1:

$$\frac{\partial U}{\partial t}+U\frac{\partial U}{\partial x}+g\frac{\partial z}{\partial x}+U|U|\phi(h)=0 \qquad (3.3)$$

Model 2:

$$\frac{\partial z}{\partial x}+\frac{Q|Q|}{C^2A^2H}+\frac{\beta}{gA}\frac{\partial Q}{\partial t}-\frac{\partial z}{\partial t}\{\frac{\beta Q}{gA^2}(b+H\frac{\partial b}{\partial z})+j\frac{(B-b)}{gA^2}Q\}$$
$$+\frac{\alpha Q}{gA^2}\frac{\partial Q}{\partial x}-\frac{\alpha Q^2}{gA^3}\frac{\partial A}{\partial x}+\frac{H}{2\gamma}\frac{\partial \gamma}{\partial x}+\frac{\beta qQ}{gA^2\delta x}-\frac{W}{\gamma H}+\frac{kQ|Q|}{2gA^2\delta x}=0 \qquad (3.4)$$

Model 3:

$$\frac{\partial z}{\partial x}=-\frac{1}{gA}\frac{\partial Q}{\partial t}-\frac{1}{C^2A^2R}|Q|Q+\frac{2B}{gA^2}Q\frac{\partial z}{\partial t} \qquad (3.5)$$

Full derivations of the above terms and how they are expressed as finite differences in the respective models can be obtained in the appropriate references (James & Horne, 1969; Hutchison, 1976; Huizinga, 1987). Models 1 and 3 both assume that the dominant forces are those due to gravity, friction and pressure. All other terms are thus omitted from the respective equations. James and Horne (1969) justify the omission of the lateral inflow term by using the same reasoning as in the continuity equation. Although Model 1 and 3 equations differ, they are essentially the same, as Model 1 uses velocity as a variable whilst Model 3 uses discharge, discharge being

merely the product of velocity and cross-sectional area. Model 1 also allows for the fact that wind set arises when wind blows over a free surface. It includes this effect by calculating the wind set at Charters Creek, extrapolating this to the confluence of the Mpate River and The Narrows, and then filtering out the 'wind tide' from the mean water level at the confluence. Model 3 allows the wind shear term to be included should it be considered significant. Model 2 is the only model which incorporates all the above forces. Model 2 uses the technique of dividing the channel cross-section into two regions:

(1) the flow region, where the major water transfer occurs;
(2) the storage region, which is relatively shallow and has negligible velocities.

The model solves both the momentum and continuity equations for the flow region. The term, F_s, due to lateral inflow from the storage region, is applicable to this model only. This term has no contribution unless the water levels are falling, which accounts for the factor 'j', in the momentum equation, which is greater than 0 only if the water levels are falling.

3.3.3 Energy

$$z_n - z_{n+1} = \frac{1}{2g}\{\alpha_{n+1}(\frac{Q_{n+1}}{a_{n+1}})^2 - \alpha_n(\frac{Q_n}{a_n})^2\} + \frac{Q_n|Q_{n+1}|}{A_n A_{n+1}}\{\frac{2\delta x_n}{(H_n+H_{n+1})C^2} + \frac{k}{2g}\} \quad \textbf{(3.6)}$$

Subscripts n and n+1 denote adjacent channel reaches.

The energy equation is used solely by model 2. When applying this model a small channel reach between the sea and the estuary mouth is defined, as it is here, where a rapid change in channel cross-sectional area occurs, this means that Bernoulli effects may become significant.

3.3.4 Solution technique

All the models use finite difference methods for the solution of the continuity and momentum equations. Models 1 and 3 use explicit techniques whilst Model 2 uses an implicit technique. The advantage of an implicit solution is that for any time step used in the iteration the solution is stable; however implicit techniques usually are more demanding on computer facilities. For both methods the solution becomes less accurate as the time step for the iteration is increased.

3.3.5 Boundary conditions

At the estuary mouth the tidal range of the water elevation relative to the Mean Lake Level is the boundary condition which is used by all the models. Flow velocity does not need to be specified at the estuary mouth. Model 2 has an additional channel reach at the estuary mouth boundary where the energy equation is solved. The solution to the energy equation is used as the boundary condition for the momentum and continuity equations. The upstream boundary conditions are as follows:

Model 1 - inflow or outflow at the confluence of the Mpate River and the Narrows depending on lake levels and wind set at Charters Creek;

Model 2 - river inflow at any specified boundary;

Model 3 - allows for three types of boundary conditions:

(1) a dead end where no discharge occurs;

(2) a river where inflow into the estuary occurs;

(3) a lake where the water levels can vary either due to exchange of water with the estuary (or with other sources), or due to wind set.

The initial conditions required for Models 2 and 3 are water level and discharge to be specified at all estuary channel reaches, whilst Model 1 requires water levels and velocities to be specified for the reaches.

3.4 REQUIREMENTS FOR SEDIMENT TRANSPORT MODELS

For sediment transport to occur certain requirements need to be met. First, a sediment source must exist; second, a transporting medium is required; and third, the motion and physical properties of the transporting medium must be such that it can initiate and sustain sediment movement. The first two requirements will be discussed briefly below, however it is the motion and physical properties of the transporting medium which must be described by a hydrodynamic model.

In the St Lucia Estuary there are three main sediment sources:

(1) marine sediment introduced into the estuary via the process of longshore drift;

(2) aeolian sediment which is blown into the estuary whenever the prevailing winds blow over the exposed banks and across the estuary;

(3) catchment-derived sediment which is brought down into the estuary via the Narrows.

Wright (1990) established a rudimentary sediment budget for the 28-month period following the September 1987 floods. From this he concluded that approximately 239×10^3 m^3 of marine sediment, 21×10^3 m^3 of catchment derived sediment, and 7×10^3 m^3 of aeolian sediment were introduced annually into the estuary. Badenhorst (1989) estimated that 200×10^3 m^3 of the marine sediment was removed annually by dredging. Other sources do exist, eg. bank erosion, but these occur sporadically and thus should not be included in the sediment transport model unless they contribute a significant quantity of sediment within a specified time period.

The physical properties of the sediment from each source, (size, density, and availability), must be determined as they will effect the mode and rate of transportation.

The second requirement for a sediment transport model is a transporting medium. The two transporting media occurring within the environs of the estuary are water and air. This study was initiated in order to determine sediment movement within the estuary mouth so aeolian transport is not considered. It is important to note that wind transports a significant volume of fine-grained sandy sediment into the estuary.

The final requirement is to describe the behaviour and properties of the transporting medium and to determine whether it can cause sediment movement. If movement is possible, then the sediment flux in all directions must be established. From the sediment fluxes areas and rates of erosion or deposition must be identified. Thus the hydrodynamic models need to specify:

(1) the flow velocity, (velocity is used rather than speed to emphasis the importance of flow direction), at all given depths and locations;

(2) turbulence effects as these enhance the sediment transporting ability;

(3) energy states of the flow at all locations as this will determine the quantity of sediment transported.

If the above can be determined then using a suitable sediment movement model, sediment transport rates can be calculated for the different modes of transport and sediment types.

3.5 SUITABILITY OF EARLIER HYDRODYNAMIC MODELS FOR LINKING TO A SEDIMENT TRANSPORT MODEL

There are essentially two assumptions made in all of the earlier models which make them unsuitable for linking to a sediment transport model. First, that the flow is one dimensional and second, that the channel reach behaves as a single body. Models 1 and 3 have additional problems associated with neglecting the effects of wind. Model 2 has drawbacks owing to the assumption that rates of flow velocity are negligible within the storage area. It must be remembered that these models were not designed for explaining sediment movement but rather for water quality, as the high lake salinity level was the original concern which caused them to be developed.

When discussing the problems associated with the assumptions incorporated into the earlier models, it must be noted that the rate of sediment transport, as well as the spatial relocation of the sediment, is of importance.

Using a one dimensional model the following problems arise.
First, flow is in uni-directional and thus sediment movement can only occur in this direction. This is clearly inadequate as secondary currents, which may deviate from the flow direction, occur and may have sufficient velocity to initiate and sustain sediment transport.

Second, the velocity is averaged for the channel cross-section, although the specific velocity at any point may vary greatly from this value. Commonly used sediment transport rate equations of Bagnold (1966), equation (2.51), Einstein (1950), equation (2.23), and Yalin (1963), equation (2.33), are all dependent on the flow velocity and thus distortion of results will occur.

The assumption that the reach behaves as a single body leads to the further problem that ebb and flood channel characteristics are ignored. Figure (3.3) shows the existence of ebb and flood channels in the study area. These features are important as they dictate the type of sediment which occurs within them, eg. fine catchment-

derived sediment is most likely to be found in the ebb channel. As mentioned previously, the type of sediment affects the mode of transport and the quantity that can be transported by a given flow velocity. The channelling of ebb and flood tidal currents also greatly changes the local flow velocity. Shoaling, in the form of flood tidal deltas, causes the channel to constrict and thus the flow velocity to increase, again distorting the results of the transport rate equations.

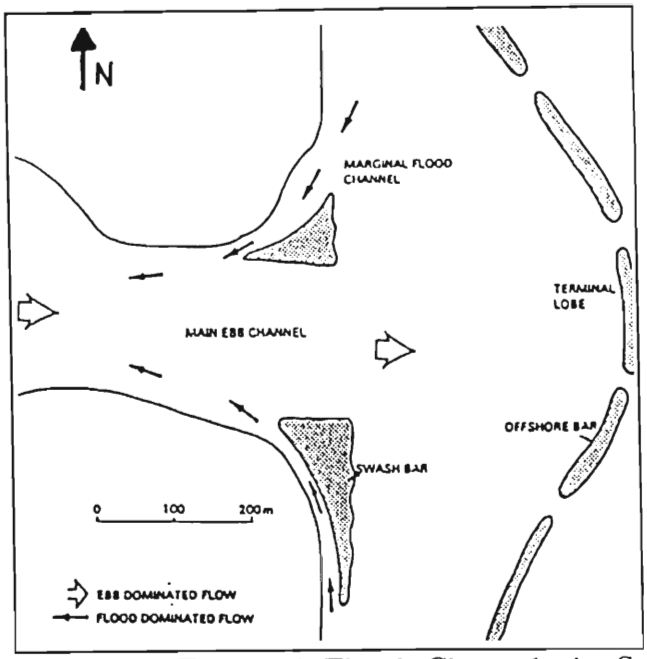

Figure 3.3 Ebb and Flood Channels in St Lucia Estuary Mouth (Wright, 1990).

Overlooking the importance of wind (models 1 and 3), creates the following problems:

(1) secondary currents caused by wind stress may move sediment directions other than the flow direction;

(2) wave energy and orientation are neglected.

In St Lucia the most common prevailing winds are southwest and northeast. To demonstrate the effect of these winds a simple observational experiment on sedimentary structures was carried out. A 20 m long and 0.1 m high sand wave was observed in Shark Basin. The sand front was staked and after two tidal cycles the sand wave's movement was noted. The front was then re-staked and the front movement noted after a further two tidal cycles. During the first period a strong southwesterly wind was blowing, thus waves moving straight into the estuary from the ocean enhanced the energy level of the flood tidal flow. During this period the sand

wave moved approximately 1 m. In the second stage there was a strong northeasterly wind, the estuary was thus protected from the wave action by the northern spit and the wind opposed the flood tidal flow, as a result the sand wave progressed only 0.1 m.

The one-dimensional hydrodynamic models discussed are inadequate for the desired purpose of linking them to a sediment transport model. The problems associated with these models could be alleviated by using a hydrodynamic model that:

(1) solves the two (horizontal) dimensional flow equations, with the vertical velocity profile being described by a velocity distribution law;

(2) is solved on a grid where flow velocity is specified for each nodal grid point, thus allowing for variations of sediment type and morphological features;

(3) includes a wind velocity factor, which specifies the effect that the wind will have on flow velocities and wave energies;

Hydrodynamic models incorporating some or all of the above do exist in various forms. Davis (1976) developed a finite element method for modelling two-dimensional unsteady flow. He applied it to tidal flow in coastal waters and wind-induced currents in shallow lakes. He assumed that the flow velocities and water densities are uniform with depth. Leendertse and Liu (1976) developed a model simulating three-dimensional flow in estuaries. Their underlying assumptions were that water movement is caused by tides, wind and pressure differences. Black (1987) developed a two-dimensional hydrodynamic model with the specific purpose of linking it to a sediment movement model and thus includes all of the above requirements. The hydrodynamic model developed in this thesis is based on these and other hydrodynmaic models. The derivation of this model is presented in the following chapter.

CHAPTER 4

DERIVATION OF THE HYDRODYNAMIC EQUATIONS

4.1 NOTATION

a	acceleration	$m.s^{-2}$
A	cross-sectional area of a unit	m^2
C_c	Chezy's coefficient	$m^{1/2}.s^{-1}$
F	force	N
g	gravitational acceleration	$m.s^{-2}$
h	free-surface elevation relative to the Mean Lake Level (MLL)	m
H	depth of bed below the (MLL)	m
H^*	hydraulic depth ($H^* = H + h$)	m
m	mass	kg
P	wetted perimeter of channel	m
R	hydraulic radius (A/P)	m
t	time	s
u	flow velocity in the x-direction	$m.s^{-1}$
v	flow velocity in the y-direction	$m.s^{-1}$
Vw	velocity of the wind	$m.s^{-1}$
ρ	density of water	$kg.m^{-3}$
ρ_a	density of air	$kg.m^{-3}$
τ	shear stress	$N.m^{-2}$

4.2 FACTORS INFLUENCING THE ST LUCIA ESTUARY

Natal Parks Board (NPB) have identified sediment movement as a problem in the management of the St Lucia Estuary Mouth and they thus need to be able to predict how the sediment will move under various flow, tidal and climatic conditions. For sediment to move, it requires a transporting medium. In the environs of the St Lucia Estuary Mouth, there are two transporting mediums, namely: air and water. According to Wright (1990), it is the latter which has the greatest effect on the estuary and it is therefore necessary to develop a hydrodynamic model of the St Lucia Estuary Mouth.

An estuary is a three dimensional body of water which is continually being influenced by numerous factors, namely:

Sea:

(i) **Tidal action**: the change in the water level between high and low tides as well as that between spring and neap tides continually changes the pressure gradient within the estuary;

(ii) **Wave action:** the orientation and energy of the waves affect the flow velocities as well as the turbulence within the estuary;

(iii) **Salinity**: changes in the concentration of the salt alters the density of the water and hence affects the pressure gradient. The salinity also affects the rate of flocculation;

(iv) **Local currents**: longshore drift, refraction and reflection affect the orientation of the flow;

Catchment

(i) **Lake levels**: these affect the discharge into the estuary;

(ii) **Farm Management**: poor farm management has resulted in increased silt concentrations in the St Lucia Lake System;

(iii) **Urbanisation**: the construction of dams and the increased demand on water supplies reduces the discharge into the estuary;

Geology: (i) **Slope Stability**: the degree to which the banks and the bed of the estuary can be eroded affects the sediment content in the water;

(ii) **Sediment**: the transportation of sediment, whether in the suspended, saltated or bed load form requires energy and this reduces the energy available for the fluid flow;

(iii) **Bed Composition**: this affects the frictional resistance opposing the flow;

Climate: (i) **Drought**: St Lucia Estuary is in an area that is characterised by dry and wet cycles which occur over several years. This affects the lake levels;

Weather: (i) **Wind**: this affects the flow velocity as well as the wave energy and orientation;

(ii) **Precipitation and Evaporation**: these affect the inflow and outflow of water from the estuary;

Biology: (i) **Flora and fauna**: these affect the chemical composition and the sediment content of the water in the estuary;

Man: (i) **Effluent**: this affects the chemical composition of the water;

(ii) **Recreational Usage**: this affects the turbulence and bank stability of the estuary.

To incorporate all these parameters into a mathematical model would make the model cumbersome. The mathematical model should simplify the situation by utilising only the dominant factors yet it must still provide a good approximation of the real situation so that, once it is refined, it can be utilised as a management tool by the NPB.

4.3 DECISION ON DIMENSIONS

As mentioned earlier, an estuary is a three dimensional body, and thus, depending on the simplification of the mathematical model used to describe its behaviour, it can be either a one-, two- or three-dimensional model.

One-dimensional models have been successfully applied to rivers and estuaries to predict flow velocities, salinity diffusion and, to a limited extent, sediment transport rates. In a one-dimensional problem the flow direction is assumed to be parallel to the river banks. However, in an estuarine environment, the opposing flow of the flood tide can create situations, where in one cross-section of the estuary, there might be two or more areas with considerably different flow velocities. Thus to predict anything more complex than the net discharge or the net inflow of saline water more than one dimension will have to be considered.

To decide between two- and three-dimensional models it is necessary to establish what causes vertical flows and whether these vertical flows will have a significant effect on the desired accuracy of the model.

It is important to note that turbulence will not be included when discussing vertical currents. This is due to the fact that movements resulting from turbulence have no net vertical movement. As can be seen in figure (2.10), when discussing Bagnold's Sediment Transport equation, the upward currents are balanced by downward currents.

Some of the main causes of vertical movements in fluids are strong salinity and temperature gradients, flow around bends, waves and wind induced tides.

Salinity: The whole St Lucia Lake System is very susceptible to variations in salinity, see figure (4.1). In dry cycles there is an influx of saline water into the system due to the reduced hydraulic head of the lake. However, during high rainfall periods the system is flushed resulting in

a low salinity, eg. a salinity of 2.5 parts per thousand (ppt) compared to the sea 36 ppt have been recorded at the jetty which is 0.5 km inland. Despite this, the salinity of the region of the estuary to be modelled (i.e. between 0.4 km and 2.0 km upstream of the sea) is fairly uniform and thus no major saline wedges are likely to develop.

Temperature: The differences in temperature between the sea and estuary are not great due to the fact that the Aghulas Current is warm and that Natal experiences a warm climate. Also, the fact that the estuary is relatively shallow, with a mean depth of 3 m in the study region, no major temperature differences are likely to be generated through insolation.

Topography: The region of the estuary to be modelled approximates a rectangular shape, see figure (3.1), and thus no large bends occur. The bed topography includes large features, eg. flood- and ebb-tidal channels. The flow in these channels is generally greater than in other areas of the estuary and thus any vertical flow is small relative to the horizontal flow.

Waves: Waves generally occur as swells within the estuary mouth, having broken on the ebb-tidal deltas before entering the mouth. The motion of individual water particles within swells is circular, see figure (4.2), and thus the net upward motion is equal to the net downward motion.

Wind: Wind blowing across large stretches of water causes a heaping effect, or wind tide, which generates a pressure gradient resulting in a circular flow, as can be seen in figure (4.3). However, in St Lucia the dominant winds are northeasterly or southwesterly, see figure (4.4), which are across the width of the estuary. The maximum width is 500 m and thus no major wind tide is likely to be generated.

For the above reasons the horizontal velocities are likely to be much greater than the vertical velocities over a time period of a tidal cycle or more. The data requirements are also much greater for a three-dimensional hydrodynamic model. The collection of this data would be extremely time consuming and expensive. Thus a two-dimensional hydrodynamical model using depth-averaged flow would probably best suit the management needs of the NPB. Having decided on a two-dimensional model it should be noted that the flow is non-uniform and unsteady.

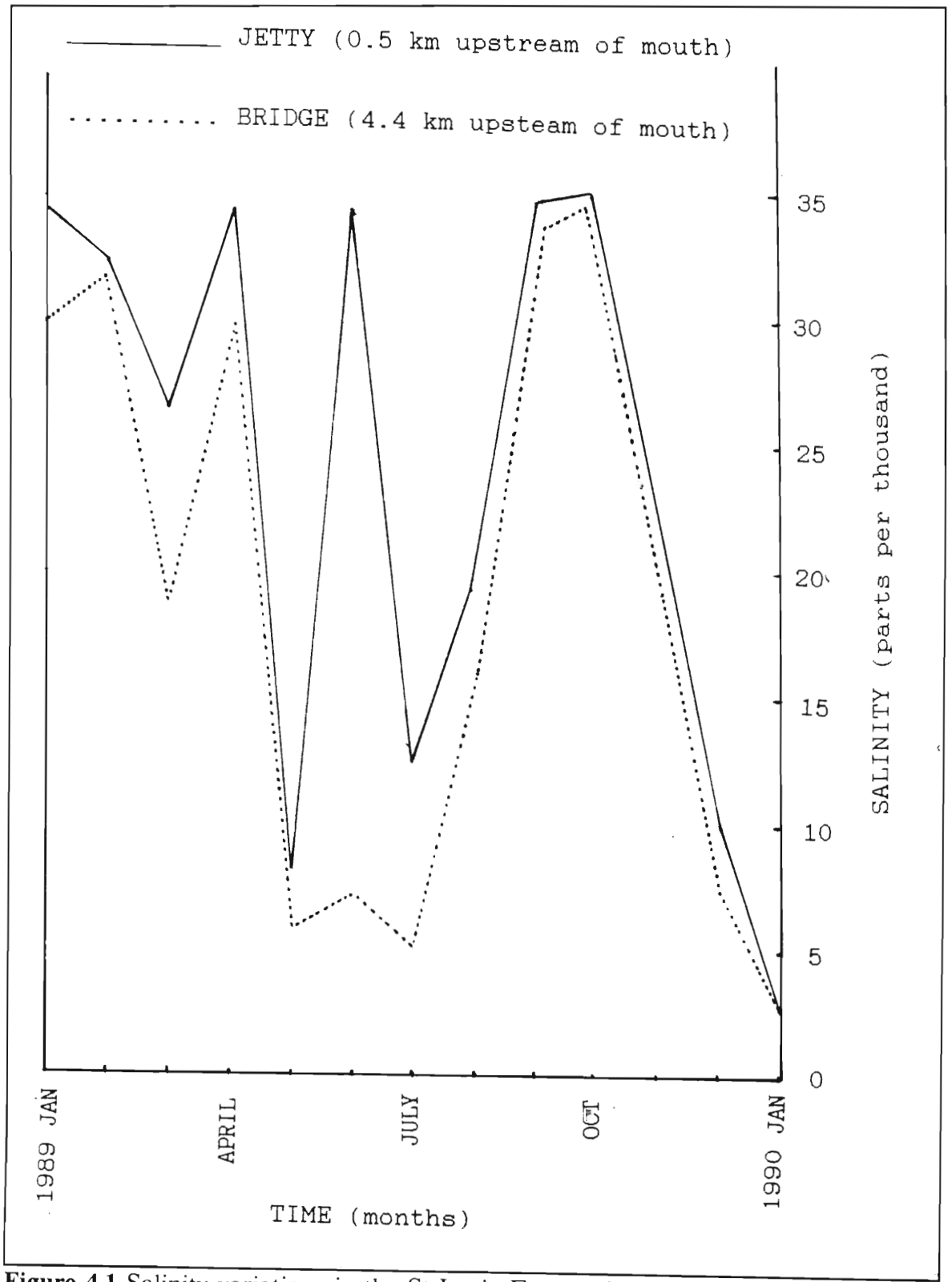

Figure 4.1 Salinity variations in the St Lucia Estuary from January 1989 to January 1990. (Data supplied by Natal Parks Board)

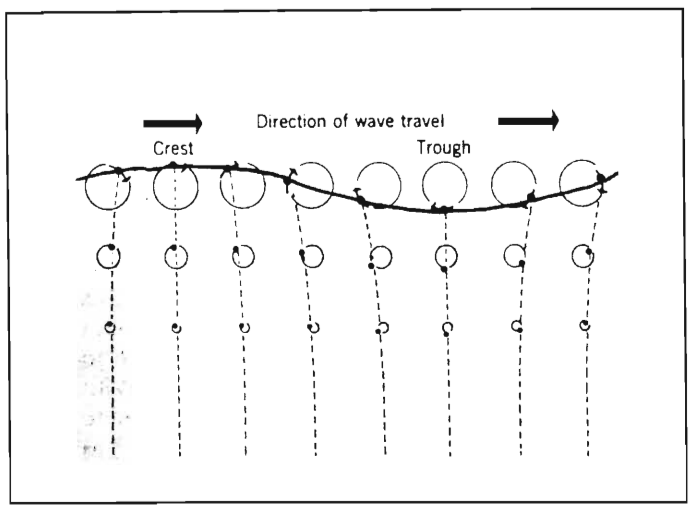

Figure 4.2 Orbital motion in waves of a relatively low height (Strahler & Strahler, 1973)

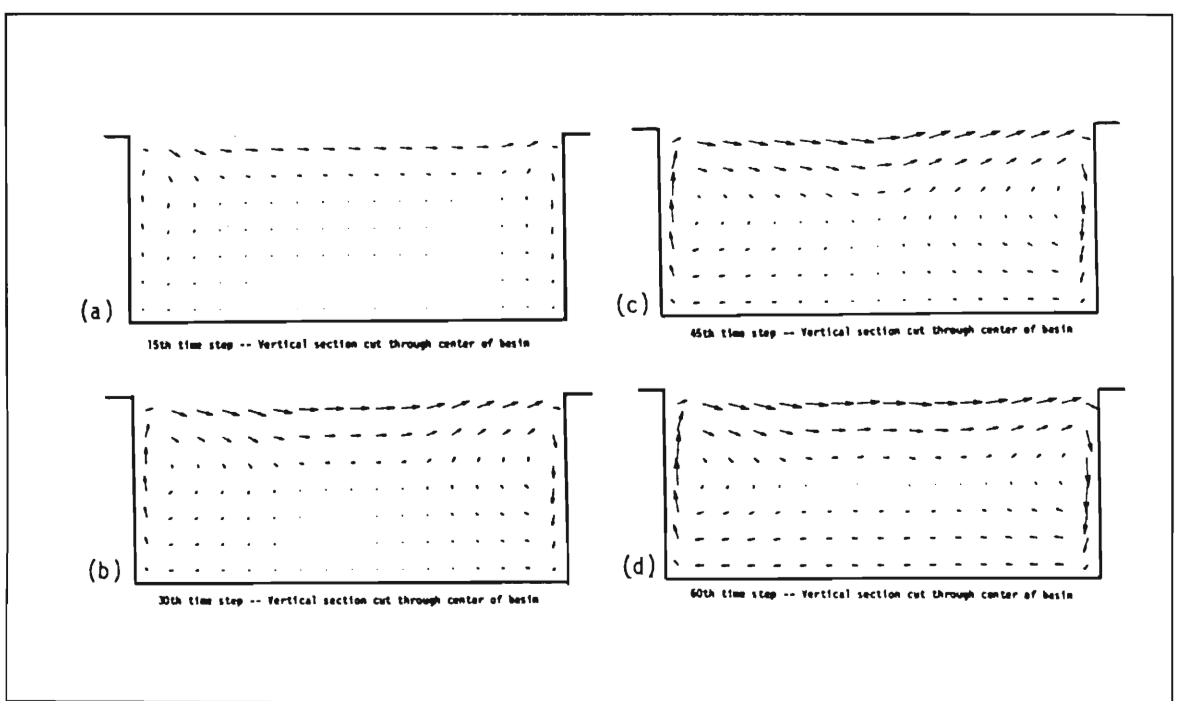

Figure 4.3 The response in a vertical cross-section of a rectangular basin under a wind stress (Leenderste & Liu, 1976)

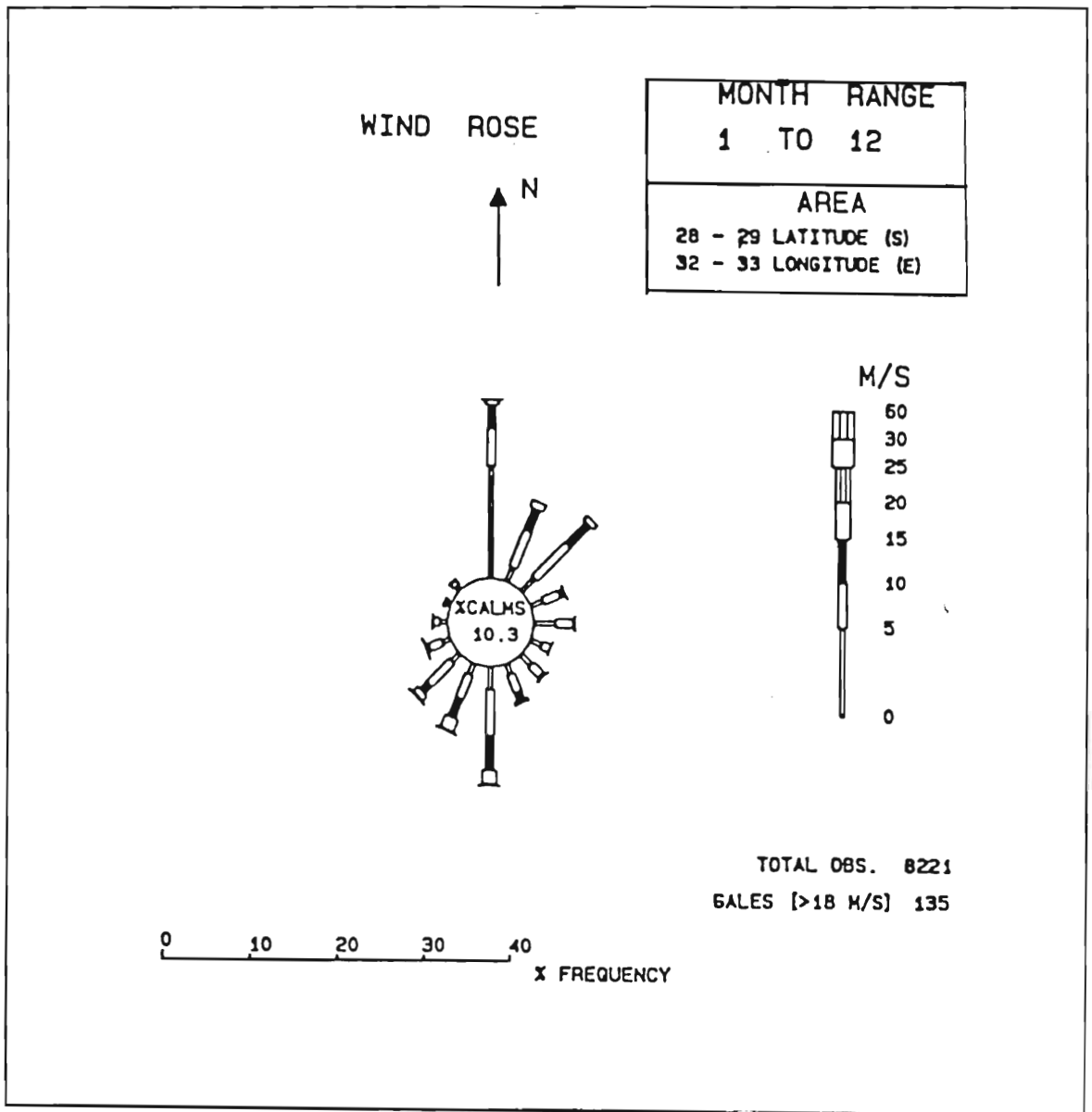

Figure 4.4 Wind rose for the St Lucia area. (Van Heerden and Swart, 1986)

4.4 DERIVATION OF THE EQUATIONS

The model is two dimensional with the velocities being averaged over the depth. The two dimensions will be in the horizontal plane with one direction taken parallel to the estuary banks, (the y-direction), and the other orthogonal to this, (the x-direction). Flow in the y-direction will be denoted by **v** and in the x-direction by **u**.

The equations which are to be the basis of this model are two fundamental laws of Physics, namely:

(i) **Newton's 2nd Law of Motion** or the conservation of momentum;

(ii) **Continuity** which is the principle that matter can neither be created nor destroyed.

4.4.1 Newton's 2nd Law

Newton's 2nd Law states that the sum of the forces acting on a body is equal to the product of the mass of the body and the acceleration of the body.

$$\sum F = ma \qquad (1)$$

As stated earlier there are numerous factors which influence an estuary. In this model only the forces that affect the physical flow conditions will be considered, and of these, only the dominant forces will be incorporated into the model.

(i) **Pressure Gradient**: If we consider a unit volume of water in a river, the water upstream of the unit exerts a pressure force on the water within the unit. Similarly, the water downstream of the unit exerts a force on the unit. Thus the net force exerted on the unit is the difference between the upstream, $\mathbf{F_u}$, and downstream, $\mathbf{F_d}$,

pressure forces. The force due to pressure can be

$$F_p = -\rho g(H + h)A \tag{4.2}$$

where **A** is the cross-sectional area of the unit, **H** the depth of the bed below the datum, which is the Mean Lake Level (MLL), and **h** the height of the free-surface relative to the MLL, ρ is the density of the water and g is the gravitational acceleration. Thus the net pressure force, $\mathbf{F_p}$, in the x-direction can be expressed as:

$$F_p = F_u - F_d = -\rho g \frac{\partial(H + h)}{\partial x}.\delta x.A \tag{4.3}$$

The product δ**x.A** is just the volume of a unit and therefore equation (4.3) can be simplified to:

$$F_p = -\rho g vol \frac{\partial(H + h)}{\partial x} \tag{4.4}$$

and in the y-direction as :

$$F_p = F_u - F_d = -\rho g vol \frac{\partial(H + h)}{\partial y} \tag{4.5}$$

(ii) **Bed Friction**: flow over a surface that is not perfectly smooth is obviously going to generate stresses. If the flow is no longer laminar then Chezy's coefficient for arbitrary shapes can be introduced. It is based on the absolute roughness, **a**, or the size of the ripples and the texture of the bed material, and the hydraulic radius, **R**, which is the cross sectional area divided by the wetted perimeter of the channel.

There is also a third term based on the thickness of the laminar sublayer, δ, however this is usually negligible in open channel flow (Abbott & Basco, 1989). Chezy's coefficient can be written as:

$$C_c = 18\,\mathrm{Log}\frac{6R}{a + \delta/7} \tag{4.6}$$

or neglecting the laminar sublayer viscous effect:

$$C_c = 18\,\mathrm{Log}\frac{6R}{a} \tag{4.7}$$

Now using Chezy's hypothesis the stress generated due to bed friction, in the x-direction is:

$$\tau_x = \frac{g\rho u \forall}{C_c^2} \tag{4.8}$$

and similarly in the y-direction is:

$$\tau_y = \frac{g\rho v \forall}{C_c^2} \tag{4.9}$$

where

$$\forall = \sqrt{u^2 + v^2} \tag{4.10}$$

Thus the force due to friction is the product of the stress and the area over which it is exerted. The area is the product of the perimeter of the channel, **P**, and the change in either the x-direction, **δx**, or y-direction, **δy**. The wetted perimeter can be written as the quotient of the cross sectional area, **A**, and the hydraulic depth, **(H + h)**. Thus the force due to bed friction in the x-direction can be written as:

$$F_{bx} = \frac{-A\delta x}{(H + h)} \cdot \frac{g\rho u \forall}{C_c^2} = -\rho vol. \frac{gu\forall}{(H + h)C_c^2} \qquad (4.11)$$

and similarly in the y-direction:

$$F_{by} = -\rho vol. \frac{gv\forall}{(H + h)C_c^2} \qquad (4.12)$$

(iii) **Wind Stress**: Wind causes a circular flow in the vertical plane and thus generates stresses both at the surface and the bed. If these two stress are assumed to be linearly related then the total wind stress, τ_w, can be written as the product of a constant, λ, and the surface wind stress, τ_{ws}. This stress is easily calculated as

$$\tau_w = \lambda \tau_{ws} = \lambda \omega^2 \rho_a V_w^2 \qquad (4.13)$$

where V_w is the wind velocity and ρ_a is the atmospheric density. ω is a constant which must be calculated using real data. At present the only data is an erratic supply from Voluntarily Observing Ships (VOS). Thus, as the goal of this project is only to indicate how the model could be used as a management tool, it has been left out of the simulation. At a later, stage a comprehensive wind data set could be collected and, the wind stress term then included in the model.

(iv) **Coriolis Force**: The Coriolis force is due to the rotation of the earth and causes particles in motion to be deflected to the left relative to the horizontal component of their velocity in the southern hemisphere. The acceleration, **a**, of a particle under the influence of the Coriolis force can be calculated as:

$$a = 2\omega v \sin\theta \tag{4.14}$$

where ω is $2\pi/86400$, (ie. one revolution in 86400 seconds) and θ is the latitude. Thus, noting that St. Lucia Estuary Mouth is at 28° S and that the maximum recorded flow is 0.7 $m.s^{-1}$, this gives an acceleration of each particle of 4.8×10^{-4} $m.s^{-2}$. From this it can be seen that the Coriolis force is negligible and it has thus been omitted from the model.

Having now identified the forces involved, the acceleration needs to be determined. Calculating the acceleration in the y-direction first, it is important to note that, **v**,is a function of both space dimensions and time, and thus should be written as **v(x,y,t)**. Thus acceleration, which is the rate of change of velocity with respect to time can be written as:

$$a = \frac{dv(x,y,t)}{dt} = \frac{\partial v}{\partial t} + \frac{\partial v}{\partial x}.\frac{\partial x}{\partial t} + \frac{\partial v}{\partial y}.\frac{\partial y}{\partial t} \tag{4.15}$$

However, $\partial x/\partial t$ is just **u** and $\partial y/\partial t$ is **v**, thus **a** can be written as:

$$a = \frac{\partial v}{\partial t} + u\frac{\partial v}{\partial x} + v\frac{\partial v}{\partial y} \tag{4.16}$$

Similarly, the acceleration in the x-direction is given as:

$$a = \frac{\partial u}{\partial t} + u\frac{\partial u}{\partial x} + v\frac{\partial u}{\partial y} \tag{4.17}$$

Thus the equations for Newton's 2nd Law are, in the x-direction and y-direction respectively:

$$-\rho g\frac{\partial(H + h)}{\partial x}vol - \frac{\rho g u \forall vol}{(H + h)C_c^2} = (\rho vol)(\frac{\partial u}{\partial t} + u\frac{\partial u}{\partial x} + v\frac{\partial u}{\partial y}) \tag{4.18}$$

$$-\rho g\frac{\partial(H + h)}{\partial y}vol - \frac{\rho g v \forall vol}{(H + h)C_c^2} = (\rho vol)(\frac{\partial v}{\partial t} + u\frac{\partial v}{\partial x} + v\frac{\partial v}{\partial y}) \tag{4.19}$$

and dividing through by the product of density and volume the equations become:

$$-g\frac{\partial(H + h)}{\partial x} - \frac{g u \forall}{(H + h)C_c^2} = \frac{\partial u}{\partial t} + u\frac{\partial u}{\partial x} + v\frac{\partial u}{\partial y} \tag{4.20}$$

$$-g\frac{\partial(H + h)}{\partial y} - \frac{g v \forall}{(H + h)C_c^2} = \frac{\partial v}{\partial t} + u\frac{\partial v}{\partial x} + v\frac{\partial v}{\partial y} \tag{4.21}$$

4.4.2 Continuity

The continuity equation is based on the fact that the average rate of inflow into a section of the estuary must equal the sum of the average rate of outflow and the average rate of increase of storage area. When deriving this equation, third order differentials are assumed to be negligible. Flow is the product of the flow velocity and the cross-sectional area. The average hydraulic depth in the x-direction, H^* is

$$H^* = (H + h) + \frac{\partial(H + h)}{2\partial y}\delta y \tag{4.22}$$

and thus the average inflow is

$$\text{average inflow} = u\delta y H^* + \frac{1}{2}\frac{\partial}{\partial t}(u\delta y H^*)\delta t \tag{4.23}$$

To determine the outflow it must be noted that the flow velocity and cross-sectional area must be calculated at a distance δx downstream. Thus the average outflow is

$$(u + \frac{\partial u}{\partial x}\delta x + \frac{1}{2}\frac{\partial u}{\partial t}\delta t)(\delta y H^* + \frac{\partial}{\partial x}(\delta y H^*)\delta x + \frac{1}{2}\frac{\partial}{\partial t}(\delta y H^*)\delta t) \tag{4.24}$$

The difference between inflow and outflow in the x-direction can be shown to be

$$\text{inflow} - \text{outflow} = -\frac{\partial}{\partial x}[u(H + h)]\delta x \delta y \tag{4.25}$$

and similarly in the y-direction

$$\text{inflow} - \text{outflow} = -\frac{\partial}{\partial y}[v(H + h)]\delta x \delta y \qquad (4.26)$$

The average rate of increase of the storage area is

$$\text{average increase of storage area} = \delta x \delta y \frac{\partial (H + h)}{\partial t} \qquad (4.27)$$

It must be noted that the depth of the bed relative to the datum (MLL) is constant with time thus $\delta(H + h)/\delta t$ is equal to $\delta h/\delta t$. Thus the continuity equation can be written as

$$-\frac{\partial}{\partial x}[u(H + h)]\delta x \delta y - \frac{\partial}{\partial y}[v(H + h)]\delta x \delta y - \delta x \delta y \frac{\partial h}{\partial t} = 0 \qquad (4.28)$$

Dividing through by $-\delta x \delta y$ the continuity equation becomes

$$\frac{\partial h}{\partial t} + \frac{\partial}{\partial x}[u(H + h)] + \frac{\partial}{\partial y}[v(H + h)] = 0 \qquad (4.29)$$

Thus the flow can be described by the equations (4.20), (4.21) and (4.29). These equations are non-linear and are not decoupled and thus need to be solved using the technique described in the next chapter.

CHAPTER 5

SOLUTION TECHNIQUE

5.1 TYPES OF NUMERICAL METHODS

There are many different ways of translating equations in the continuum to equations which can be dealt with by a computer. A computer can only manipulate discrete bits of information and thus a numerical solution must create an illusion of continuity by using a series of finite values. The principal numerical methods being used in Computational Fluid Dynamics at present are:

(1) Finite-difference Methods (FDM);
(2) Finite-element Methods (FEM);
(3) Method of Characteristics (MOC).

In the case of FDMs, the continuum of space is divided into a series of fixed grid points. Hydrodynamic equations are then written so that derivatives are approximated by Taylor series expansions. The number of terms used depends on the desired accuracy of the model. These equations are then solved using fixed time intervals. The equations can be solved by either using explicit or implicit techniques. Explicit techniques are the simplest but short wave oscillations can occur due to the non-linear terms, and stability conditions restrict the time step used. This will be discussed in more detail later. Implicit techniques are more complex and difficult to compute but are inherently stable, thus enabling a greater time step to be used.

In the case of FEMs, the space continuum is divided into discrete elements centred around nodal points, see figure (5.1) (Abbott & Basco, 1989). The value of any space dependent variable is specified at the nodal points and the value at any intermediate point can be calculated by using any linear or higher-order polynomial interpolation. The values of the variables are fixed at the nodal points, thus the spatial derivatives at these points are zero. The spatial derivatives for an element are formed by

looking at the derivatives of the variable on either side of the nodal point. The advantages of this method are that the elements can be designed to fit complex boundary shapes and the size of elements can be altered in areas of the estuary where greater detail is required (McDowell, 1976). The equations are however, more complex than those obtained when using FDMs and consequently require more computing time.

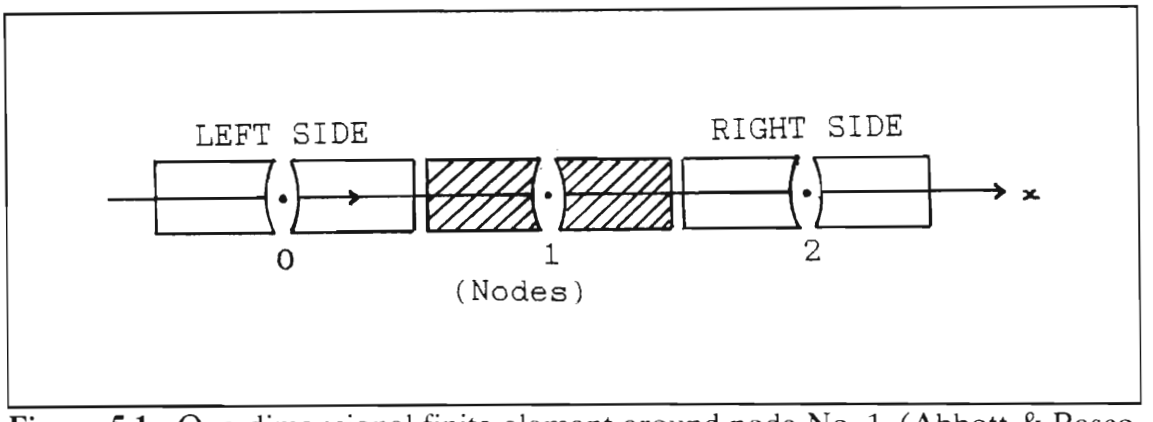

Figure 5.1 : One-dimensional finite element around node No. 1. (Abbott & Basco, 1989)

The MOC begins with a fixed grid but computations are then advanced along characteristic lines in the space-time plane. Solutions are obtained where characteristic lines from different ends of the grid intersect. These points of intersection can occur anywhere within the area for which a solution is being sought and at these points data is required. This makes it necessary to collect and store large quantities of data.

The computer facilities available for this project were limited to an 80826 IBM compatible PC. Thus the FDM was selected as it is the simplest to develop and requires the least data points.

5.2 FINITE-DIFFERENCE NUMERICAL METHOD

The actual finite difference technique used in the model that has been developed is an Alternating Direction Implicit (ADI) technique. The ADI method was originally put forward by Peaceman and Rachford (1955). This is a scheme that is decomposed into two steps, or in other words, the time operator is split into two time steps, **t = n + 1/2** and **t = n + 1**. Each step solves the hydrodynamic equations along lines parallel to the x - and y - directions. The solutions of these equations involve setting up and solving a pent-diagonal matrix equation. The actual solution of the pent-diagonal matrix equation in each step is based on the Preissmann Scheme. According to Abbott & Basco (1989), Preissmann invented this implicit finite-difference scheme in 1960 for the solution of one dimensional open-channel hydraulics problems. Preissmann's operator is a 4 - point operator, where for any flow dependent variable, **f**, which is a function of space and time i.e. **f(x,t)** the approximations to continuity are as follows:

$$\frac{\partial f(x,t)}{\partial t} \approx (1 - \varphi)\frac{f_i^{n+1} - f_i^n}{\Delta t} + \varphi\frac{f_{i+1}^{n+1} - f_{i+1}^n}{\Delta t} \qquad (5.1)$$

$$\frac{\partial f(x,t)}{\partial x} \approx (1 - \Theta)\frac{f_{i+1}^n - f_i^n}{\Delta x} + \Theta\frac{f_{i+1}^{n+1} - f_i^{n+1}}{\Delta x} \qquad (5.2)$$

where φ and θ are in the range [0,1] and the points at the time step **n** are known. The superscripts denote the time coordinate and the subscript the spatial coordinate. By taking $\varphi = 1/2$ and $\theta = 1/2$ equal weighting is given to the different values. The equations (4.20), (4.21) and (4.29) are hyperbolic as can be seen by the terms $u.\partial u/\partial x$, $v.\partial v/\partial y$ etc. In order to apply Preissmann's Scheme the equations must be linearised. This is done by giving **u**, **v** and **h** approximate values based on predicted values at the next time step, obtained by linear extrapolation, values in adjacent grid points, and the present values:

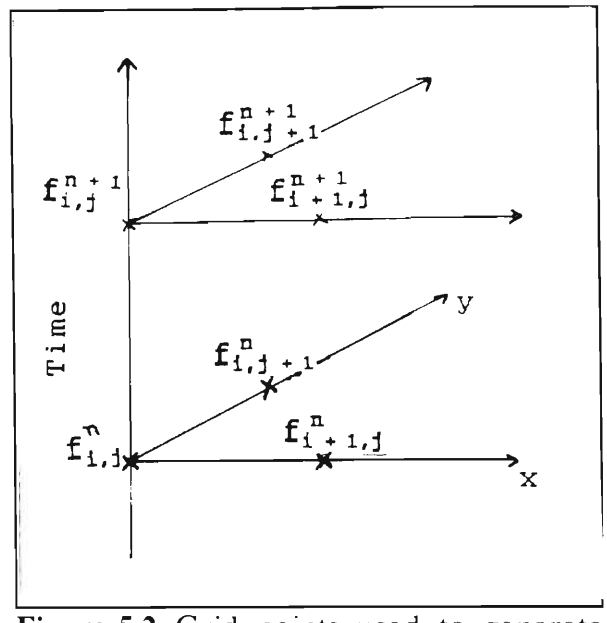

Figure 5.2 Grid points used to generate approximations.

$$f^{*}_{i,j} = \frac{f^{n+1}_{i,j} + f_{i,j} + f^{n+1}_{i+1,j} + f^{n}_{i+1,j} + f^{n+1}_{i,j+1} + f^{n}_{i,j+1}}{6} \qquad (5.3)$$

where **f** is any of the variables **u**, **v** or **h** and **f*** is the approximate value, see figure (5.2).

Equations (4.20), (4.21) and (4,29) now become

$$-g\frac{\partial(H+h)}{\partial x} - \frac{gu^{*}\forall}{(H+h)C_c^2} = \frac{\partial u}{\partial t} + u^{*}\frac{\partial u}{\partial x} + v^{*}\frac{\partial u}{\partial y} \qquad (5.4)$$

$$-g\frac{\partial(H+h)}{\partial y} - \frac{gv^{*}\forall}{(H+h)C_c^2} = \frac{\partial v}{\partial t} + u^{*}\frac{\partial v}{\partial x} + v^{*}\frac{\partial v}{\partial y} \qquad (5.5)$$

$$\frac{\partial h}{\partial t} + u^{*}\frac{\partial(H+h)}{\partial x} + (H+h^{*})\left(\frac{\partial u}{\partial x} + \frac{\partial v}{\partial y}\right) + v^{*}\frac{\partial(H+h)}{\partial y} = 0 \qquad (5.6)$$

Equations (5.4), (5.5) and (5.6) are not decoupled (in other words the variables **u**, **v** and **h** occur in all three equations). To overcome this, when solving the equations parallel to the x - direction, the variables in the y - direction are kept constant with time and similarly, when solving along the lines parallel to the y - direction, the variables in the x - direction are kept constant with time. This means that in the first time step, **t = n** to **t = n + 1/2**,where **t** is the time coordinate, equations (5.4) and (5.6) can be solved using the double sweep implicit method, and equation (5.5) can be solved explicitly. Similarly during the second time step, **t = n + 1/2** to **t = n + 1**, equation (5.4) is solved explicitly and the double sweep method is used to solve equations (5.5) and (5.6), see figure (5.3). Only the solution method for the first time step is discussed in the following sections as the solution method for the second time step is similar.

5.2.1 The Double Sweep Method

Using the implicit method for equations (5.4) and (5.6) requires the solution of either a pent-diagonal or hept-diagonal matrix depending on whether a forward-difference or central-difference scheme is used. A forward-difference operator is

$$\frac{\partial f}{\partial g} \approx \frac{f_{i+1} - f_i}{\Delta g} \qquad (5.7)$$

Where **f** is any function dependent on the variable **g**, and where the subscripts are the coordinates for the variable **g**. Using the same notation a central-difference operator is

$$\frac{\partial f}{\partial g} \approx \frac{f_{i+1} - f_{i-1}}{2\Delta g} \qquad (5.8)$$

The advantage of using a central difference scheme is that the truncation error order is $O(\Delta t^2, \Delta x^2, \Delta y^2)$, provided that values are equally weighted between the time

coordinates **n** and **n + 1/2** during the first time step and **n + 1/2** and **n + 1** during the second time step. The disadvantage of the hept-diagonal scheme is that it is more complex than the pent-diagonal scheme. The forward difference scheme has been used in this model and it has a truncation error of order $O(\Delta t,\Delta x,\Delta y)$.

Using the approximations described in equation (5.3) to linearise the equations and the Preissmann Scheme with $\varphi = 1/2$ and $\theta = 1/2$ the equations (5.4) and (5.6) can be rewritten as follows:

$$\frac{(u_{i,j}^{n+1/2} - u_{i,j}^{n} + u_{i+1,j}^{n+1/2} - u_{i+1,j}^{n})}{\frac{2\Delta t}{2}} +$$
$$u_{i,j}^{*}\frac{(u_{i+1,j}^{n+1/2} - u_{i,j}^{n+1/2} + u_{i+1,j}^{n} - u_{i,j}^{n})}{2\Delta x} + \qquad (5.9)$$
$$g\frac{(2H_{i+1,j} - 2H_{i,j} + h_{i+1,j}^{n+1/2} - h_{i,j}^{n+1/2} + h_{i+1,j}^{n} - h_{i,j}^{n})}{2\Delta x} +$$
$$v_{i,j}^{*}\frac{(u_{i,j+1}^{n} - u_{i,j}^{n})}{\Delta y} = -\frac{g u_{i,j}^{*}\forall}{(H_{i,j} + h_{i,j}^{*})C_c^2}$$

and

$$\frac{(h_{i,j}^{n+1/2} - h_{i,j}^{n} + h_{i+1,j}^{n+1/2} - h_{i+1,j}^{n})}{\frac{2\Delta t}{2}} +$$
$$(H_{i,j} + h_{i,j}^{*})\frac{(u_{i+1,j}^{n+1/2} - u_{i,j}^{n+1/2} + u_{i+1,j}^{n} - u_{i,j}^{n})}{2\Delta x} + \qquad (5.10)$$
$$u_{i,j}^{*}\frac{(2H_{i+1,j} - 2H_{i,j} + h_{i+1,j}^{n} - h_{i,j}^{n} + h_{i+1,j}^{n+1/2} - h_{i,j}^{n+1/2})}{2\Delta x} +$$
$$v_{i,j}^{*}\frac{(H_{i,j+1} - H_{i,j} + h_{i,j+1}^{n} - h_{i,j}^{n})}{\Delta y} + (H_{i,j} + h_{i,j}^{*})\frac{(v_{i,j+1}^{n} - v_{i,j}^{n})}{\Delta y} = 0$$

Equations (5.9) and (5.10) can be re-written as

$$A1\,U_{i,j}^{n+1/2} + B1\,h_{i,j}^{n+1/2} + C1\,U_{i+1,j}^{n+1/2} + D1\,h_{i+1,j}^{n+1/2} = E1_{i,j} \tag{5.11}$$

$$A2\,U_{i,j}^{n+1/2} + B2\,h_{i,j}^{n+1/2} + C2\,U_{i+1,j}^{n+1/2} + D2\,h_{i+1,j}^{n+1/2} = E2_{i,j} \tag{5.12}$$

where

$$\begin{aligned}
A1 &= \frac{1}{2} - U_{i,j}^{*}\frac{\Delta t}{4\Delta x} \\
B1 &= -g\frac{\Delta t}{4\Delta x} \\
C1 &= \frac{1}{2} + U_{i,j}^{*}\frac{\Delta t}{4\Delta x} = 1 - A1 \\
D1 &= g\frac{\Delta t}{4\Delta x} = -B1 \\
E1 &= \frac{1}{2}(u_{i,j}^{n} - u_{i+1,j}^{n}) + u_{i,j}^{*}\frac{\Delta t}{4\Delta x}(u_{i,j}^{n} - u_{i+1,j}^{n}) + \\
&\quad g\frac{\Delta t}{4\Delta x}(2H_{i,j} - 2H_{i+1,j} + h_{i,j}^{n} - h_{i+1,j}^{n}) + \\
&\quad v_{i,j}^{*}\frac{\Delta t}{2\Delta y}(u_{i,j}^{n} - u_{i,j+1}^{n}) - \frac{\Delta t}{2}\frac{g u_{i,j}^{*}\forall}{(H_{i,j} + h_{i,j}^{*})C_c^2}
\end{aligned} \tag{5.13}$$

and where

$$
\begin{aligned}
A2 &= -\frac{\Delta t}{4\Delta x}(H + h^*) \\
B2 &= \frac{1}{2} - \frac{\Delta t}{4\Delta x}u^* \qquad = A1 \\
C2 &= \frac{\Delta t}{4\Delta x}(H + h^*) \qquad = -A2 \\
D2 &= \frac{1}{2} + \frac{\Delta t}{4\Delta x}u^* \qquad = 1 - A1 \\
E2 &= \frac{1}{2}(h_{i,j}^n - h_{i+1,j}^n) + (H_{i,j} + h_{i,j}^*)\frac{\Delta t}{4\Delta x}(u_{i,j}^n - u_{i+1,j}^n) + \\
&\quad u_{i,j}^*\frac{\Delta t}{4\Delta x}(2H_{i,j} - 2H_{i+1,j} + h_{i,j}^n - h_{i+1,j}^n) + \\
&\quad v_{i,j}^*\frac{\Delta t}{2\Delta y}(H_{i,j} - H_{i,j+1} + h_{i,j}^n - h_{i,j+1}^n) + \\
&\quad (H_{i,j} + h_{i,j}^*)\frac{\Delta t}{2\Delta y}(v_{i,j}^n - v_{i,j+1}^n)
\end{aligned}
\tag{5.14}
$$

Thus the following pent-diagonal matrix equation needs to be solved

$$
\begin{bmatrix}
A1_1 & B1_1 & C1_1 & D1_1 & 0 & 0 & \dots & \dots & \dots & 0 \\
A2_1 & B2_1 & C2_1 & D2_1 & 0 & 0 & \dots & \dots & \dots & 0 \\
0 & 0 & A1_2 & B1_2 & C1_2 & D1_2 & 0 & 0 & \dots & 0 \\
0 & 0 & A2_2 & B2_2 & C2_2 & D2_2 & 0 & 0 & \dots & 0 \\
\vdots & \vdots & \vdots & \vdots & \vdots & \vdots & \vdots & \vdots & \vdots & \vdots \\
\vdots & \vdots & \vdots & \vdots & \vdots & \vdots & \vdots & \vdots & \vdots & \vdots \\
0 & 0 & \dots & \dots & \dots & 0 & A1_I & B1_I & C1_I & D1_I \\
0 & 0 & \dots & \dots & \dots & 0 & A2_I & B2_I & C2_I & D2_I
\end{bmatrix}
\cdot
\begin{bmatrix}
u_1^{n+1/2} \\ h_1^{n+1/2} \\ u_2^{n+1/2} \\ h_2^{n+1/2} \\ \vdots \\ \vdots \\ u_I^{n+1/2} \\ h_I^{n+1/2}
\end{bmatrix}
=
\begin{bmatrix}
E1_1 \\ E2_1 \\ E1_2 \\ E2_2 \\ \vdots \\ \vdots \\ E1_I \\ E2_I
\end{bmatrix}
\tag{5.15}
$$

where the subscript is the spatial coordinate in the x-direction and I is the number of grid points in the x - direction.

Now the new variables **F1** and **G1** are introduced so that **u** and **h** are linearly related as follows:

$$u_{i,j}^{n+1/2} = F1_{i,j} h_{i,j} + G1_{i,j} \tag{5.16}$$

At **i = 1**, **u** is known for all time, thus to ensure linear independence of **u** and **h** at this boundary

$$\begin{aligned} F1_{1,j} &= 0 \\ G1_{1,j} &= u_{1,j}^{n+1/2} \qquad\qquad j \in [1;dim2] \end{aligned} \tag{5.17}$$

By substituting the right hand side of equation (5.16) into equations (5.11) and (5.13) and by carrying out suitable manipulations the $\mathbf{h}_{i,j}^{n+1/2}$ terms can be eliminated thus, the following recursive equations for **F1** and **G1** can be derived:

$$F1_{i+1,j} = \left[\frac{(A1F1 + B1)(E2 - A2G1) - (A2F1 + B2)D1}{(A2F1 + B2)C1 - (A1F1 + B1)C2} \right] \tag{5.18}$$

$$G1_{i+1,j} = \left[\frac{(A2F1 + B2)(E1 - A1G1) - (A1F1 + B1)(E2 - A2G1)}{(A2F1 + B2)C1 - (A1F1 + B1)C2} \right] \tag{5.19}$$

All subscripts, which are the spatial coordinates, are $_{i,j}$ unless otherwise stated. This recursive operation forms the first sweep from **i = 1** to **i = I**.

At **i = I**, **h** is known for all time and thus **u** can be calculated at **i = I** from equation (5.16)

$$u_{I,j}^{n+1/2} = F1_{I,j} h_{I,j}^{n+1/2} + G1_{I,j} \tag{5.20}$$

Now, by substituting equation (5.16) into (5.11) and making $\mathbf{h}_{I,J}^{n+1/2}$ the subject of the formula the following recursive equation for **h** is obtained:

$$h_{i,j}^{n+1/2} = \frac{[-C1_{i,j} u_{i+1,j}^{n+1/2} - D1_{i,j} h_{i+1,j}^{n+1/2} + E1_{i,j} - A1_{i,j} G1_{i,j}]}{[A1_{i,j} F1_{i,j} + B1_{i,j}]} \tag{5.21}$$

and hence the recursive equation for u is

$$u_{i,j}^{n+1/2} = F1_{i,j} h_{i,j}^{n+1/2} + G1_{i,j} \tag{5.22}$$

Thus all values for **u** and **h** can be calculated. This recursive operation forms the second sweep from **i = I** to **i = 1**. Note that during the second sweep, $\mathbf{u}_{1,J}^{n+1/2}$ should not be recalculated as it is defined here. It is important to note that this double sweep operation is done for j in the range [1,dim2]. In the above derivation the subscript **j** has been omitted where it is not necessary in order to simplify the derivation of equations. There is no superscript necessary for **H** as the depth of the estuary bed below Mean Lake Level (MLL) is assumed to be constant.

5.2.2 Explicit Method

Assuming that variables in the y - direction are fixed with time, equation (5.5) can be rewritten as

$$\frac{(v_{i,j}^{n+1/2} - v_{i,j}^{n})}{\Delta\frac{t}{2}} + u_{i,j}^{*}\frac{(v_{i+1,j}^{n} - v_{i,j}^{n})}{\Delta x} + v_{i,j}^{*}\frac{(v_{i,j+1}^{n} - v_{i,j}^{n})}{\Delta y} +$$
$$g\frac{(H_{i,j+1} - H_{i,j} + h_{i,j+1}^{n} - h_{i,j}^{n})}{\Delta y} = -\frac{g v_{i,j}^{*} \forall}{(H_{i,j} + h_{i,j}^{*})C_c^2} \qquad (5.23)$$

Rearranging equation (5.23), **v** can be solved for all $\mathbf{i} \in$ **[1,dim1]** and $\mathbf{j} \in$ **[1,dim2]** by the following

$$v_{i,j}^{n+1/2} = v_{i,j}^{n} - u_{i,j}^{*}\frac{\Delta t}{2\Delta x}(v_{i+1,j}^{n} - v_{i,j}^{n}) - v_{i,j}^{*}\frac{\Delta t}{2\Delta y}(v_{i,j+1}^{n} - v_{i,j}^{n})$$
$$+ g\frac{\Delta t}{2\Delta y}(H_{i,j} - H_{i,j+1} + h_{i,j}^{n} - h_{i,j+1}^{n}) - \frac{\Delta t}{2}\frac{g v_{i,j}^{n} \forall}{(H_{i,j} + h_{i,j}^{*})C_c^2} \qquad (5.24)$$

5.3 CONSTANTS

5.3.1 Depth of the bed below the Mean Lake Level

The region of the St Lucia Estuary Mouth that is being modelled is approximately rectangular. The maximum depth of the bed below the MLL within the modelled region of the estuary is 6 m according to the Anderson & Huizinga (1990). However this occurs in a narrow channel. The model which has been developed cannot cope with large changes in depth over a single grid spacing **Δx**, which is 50 m in the

simulations that have been run, without making the time step very small. Thus, as the aim of this study is to establish a model that with time and a good data set could be refined and used on the St Lucia Estuary the depth was averaged over each grid cell, thus resulting in the depth ranging from 1.6 m to 2.2 m, see figure (5.3). The location of features such as ebb and flood tidal channels was obtained from Anderson & Huizinga (1990).

5.3.2 Absolute Roughness

According to Abbott & Basco (1989) Chezy's resistance coefficient, C_c, can be calculated by the following formula when using the metric system:

$$C_c = 18\log\frac{6R}{a + \frac{\delta}{7}} \qquad (5.25)$$

where **R** is the hydraulic radius, **δ** is the thickness of the laminar sublayer and **a** is the absolute roughness or ripple height. According to Anderson & Huizinga (1990) the absolute roughness within the modelled section of the estuary is approximately 0.06 m and it was assumed that this value would remain comstant. The thickness of the laminar sublayer, **δ**, is directly proportional to the kinematic viscosity and inversely proportional to the shear velocity and is usually very small relative to the absolute roughness. Thus the **δ/7** term can be omitted from equation (5.25).

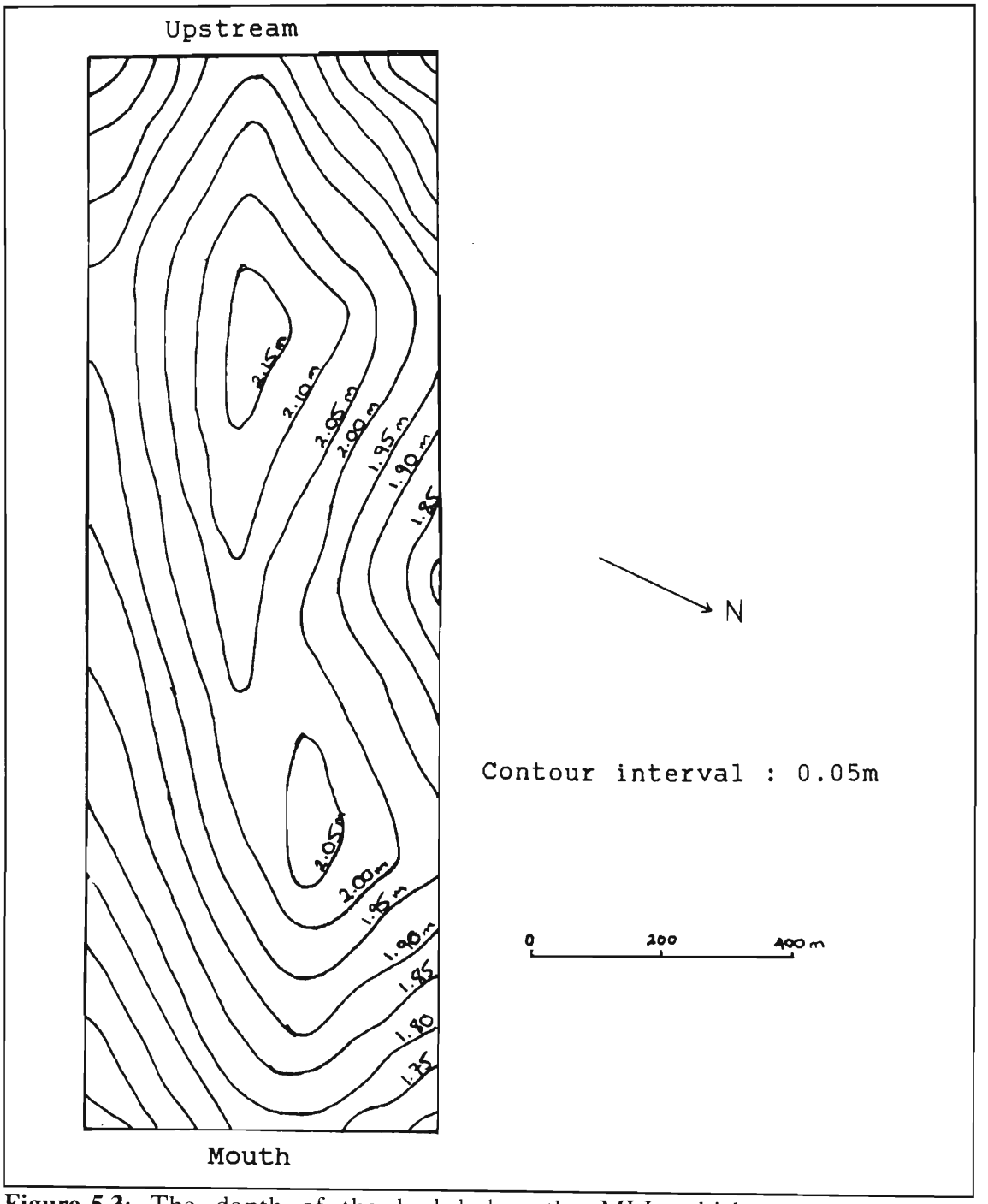

Figure 5.3: The depth of the bed below the MLL which was used in the simulations.

5.4 INITIAL CONDITIONS

Time **t = 0** for the model is taken as that time half way between high tide and low tide for the sea at the St Lucia Estuary Mouth.

5.4.1 Initial Free-surface elevation

The elevation of the free-surface ranges from 0.62 m at the downstream side of the estuary, to 0.59 m at the upstream side of the estuary. These values are based on the recordings taken by the CSIR on 11 March 1989 (Anderson & Huizinga, 1990). The recordings were taken at the mouth and at the bridge which is located 5 km from the mouth. These records were then linearly interpolated for the modelled region.

5.4.2 Initial Velocity

No continuous recordings of the water velocity occur as up until now only one-dimensional hydrodynamic models have been used on the St Lucia Estuary and these usually use discharge as opposed to flow velocity. Wright (1990) recorded velocities for a full tidal cycle at spring tide. The maximum flood-tidal velocity was $+0.7\ m.s^{-1}$ and maximum ebb-tidal velocity was $-0.4\ m.s^{-1}$. (Note that flow from the estuary to the sea is taken as positive, +, and from the sea into the estuary as negative, -). These values were used as guidelines. However, the initial velocities used in this model were generated by looking at the discharge recorded by the CSIR on 11 March 1989 (Anderson & Huizinga, 1990) and then a mean flow velocity for a given cross-section was calculated by dividing the discharge by the cross-sectional area of the estuary. In general the flow is greater in the deeper regions of the estuary. Thus the mean flow velocity was increased or decreased by comparing the depth at a given grid point to the mean cross-sectional depth. The actual formula for doing this is

$$vel_{i,j} = \frac{f_j}{A_j}\left(1 + \frac{0.5(H_{i,j} + h_{i,j} - \overline{H}_j)}{\overline{H}_j}\right) \qquad (5.26)$$

where $\mathbf{f_j}$ is the flow velocity, $\mathbf{A_j}$ is the cross-sectional area and $\mathbf{H_j}$ is the mean cross-sectional depth of the bed below the MLL for cross-section **j**. This initial flow velocity is then broken down into two components, one parallel to the x - direction and one to the y - direction. The values of these are based on the flow orientations depicted by Wright (1990).

5.5 BOUNDARY CONDITIONS

At each boundary, one of the three variables **u**, **v** or **h** has to be specified. At the upstream side of the estuary **v** is specified. On both banks of the estuary, **u** is assumed to be 0. This is because it is assumed there is no inflow to or outflow from the estuary other than from the lake system and the sea. At the banks, **v** does not have to be 0, or in other words, full slip boundary conditions are used. At the downstream side of the estuary the free-surface levels are specified. When solving for either **u** or **v** explicitly, the predicted values are used on the boundaries where values are not specified.

5.5.1 Free-surface

The free-surface is specified at the downstream side of the estuary. Due to the tides, the water-levels at the sea form a sinusoidal curve, see figure (5.4). However, the effects of the changing tide take a while to propagate up the estuary. Thus, there is a phase shift of the free-surface curve within the estuary.

The boundary values of the free-surface levels can be written as follows:

$$h(t) = -\alpha \sin(\sigma t + \phi) + \beta \qquad (5.27)$$

where α is the amplitude, which is half the difference between the free-surface level at high tide and at low tide; σ is a constant which converts time in seconds to an

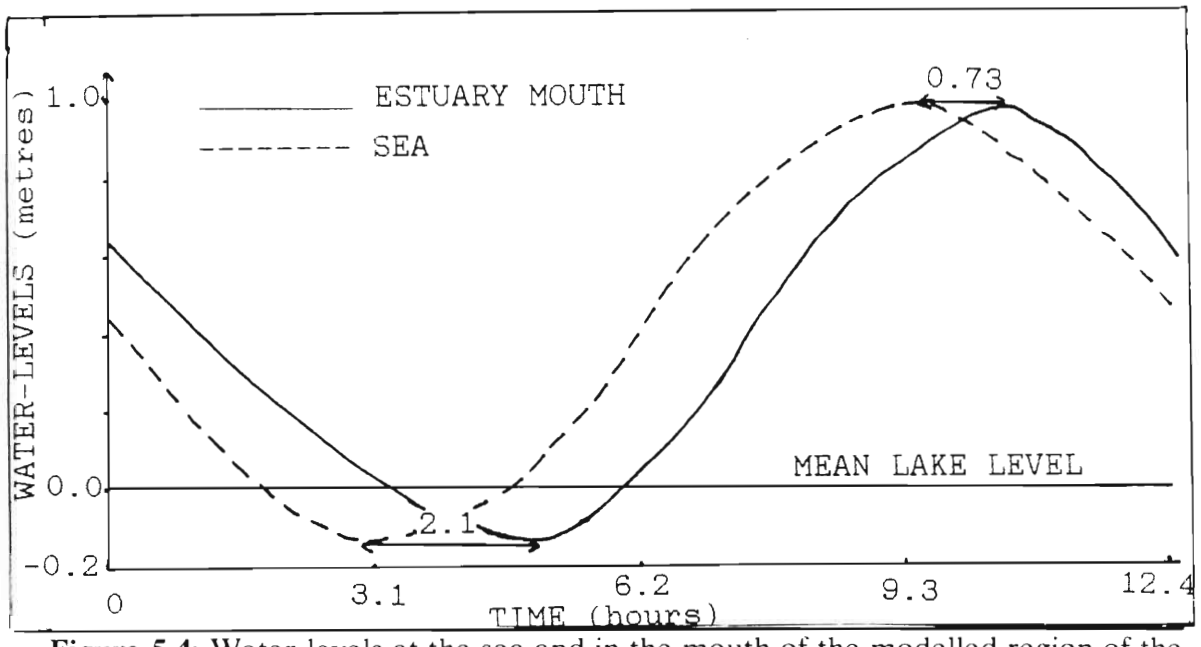

Figure 5.4: Water-levels at the sea and in the mouth of the modelled region of the estuary (Anderson & Huizinga, 1990).

angle in radian measure; ϕ is the phase shift; and β is the datum, which is the mean of the free-surface values at high tide and low tide.

The St Lucia Estuary was ebb-tidal dominated when the recordings were taken, thus the phase shift, ϕ, was not constant throughout the tidal cycle. It can be seen in figure (5.4) that on 11 March 1989, there was a phase shift of 2 hours 06 minutes at low tide whilst only 44 minutes at high tide. To cope with this, the phase shifts at high and low tides are specified, and then the phase shift at any other time is calculated by doing a linear interpolation.

5.5.2 Flow Velocity

The flow of water within the estuary does not change in synchronisation with the tides due to the momentum of the water. Depending on the lake levels, the estuary will either be flood-tidal dominated if the lake levels are lower than the sea level or ebb-tidal dominated if the lake levels are high relative to the sea. Although the flow velocities are cyclical a sinusoidal curve is not suitable for the description of the flow velocity, see figure (5.5).

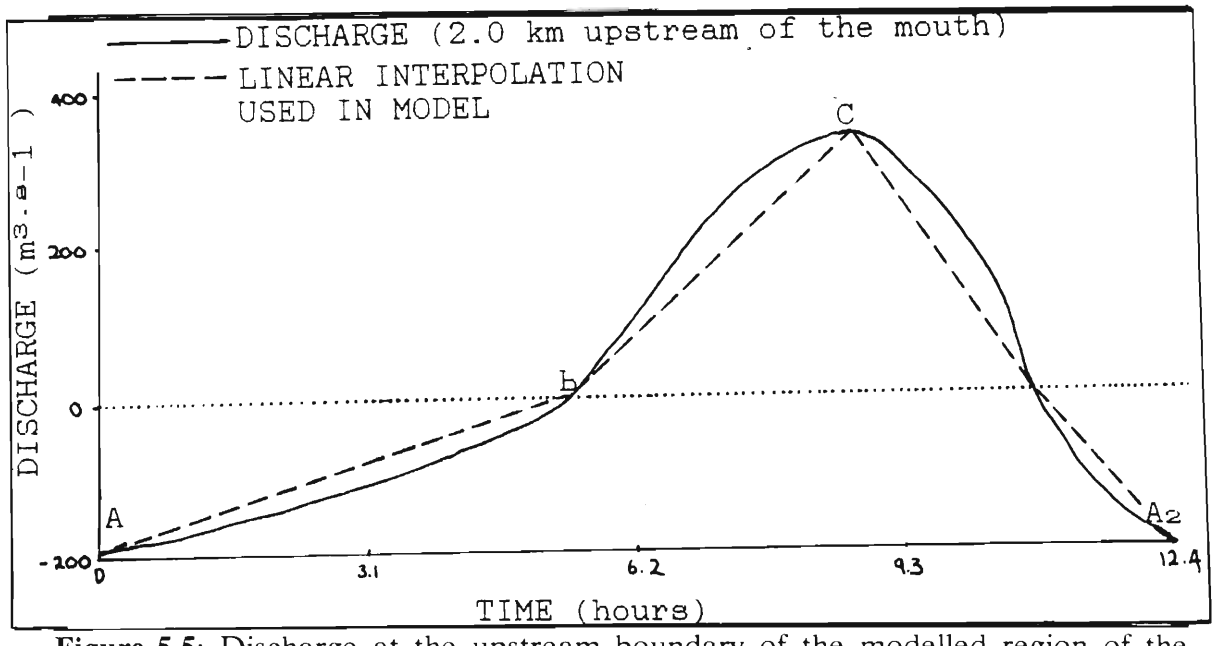

Figure 5.5: Discharge at the upstream boundary of the modelled region of the estuary (Anderson & Huizinga, 1990).

The model uses a series of linear relationships for the flow velocity. This requires that the minimum and maximum flow velocities are specified as well as the following times, see figure (5.5): **A**, the time taken from low tide at sea to that when a reversal in flow direction is noted in the estuary; **B**, the delay after low tide at sea before the maximum flow velocity is recorded in the estuary; **C**, the time taken from high tide at sea to that time when a reversal in flow direction is noted in the estuary; and **D**, the delay after high tide at sea before the minimum flow velocity is recorded in the estuary. The curve is then broken into a series of straight lines AB, BC, CD and DA_2 (where A_2 is the time taken from low tide at sea to that when a reversal in flow direction is noted in the estuary during the following tidal cycle). Linear interpolation is then used to determine the flow velocity at intermediate times.

As no data have been collected with regard to the change in orientation of the flow throughout a tidal cycle the orientation used in the model is fixed, although reversals of 180° occur as the flow changes from ebb-tidal to flood-tidal flow.

5.6 STABILITY

For the explicit solution to be stable the Courant Number, C_r, must be less than or equal to one. The Courant-Friedrichs-Lewy, (CFL), condition interprets the Courant Number as the ratio of the analytically calculated celerity of propagation, **c**, to the numerically calculated celerity of propagation $\Delta s/\Delta t$. This ensures that calculated values at a future time do not use values outside their domain of dependence, which is determined from the characteristics. In an estuary, tidal disturbances travel with a celerity which according to McDowell *& O'Connor* (1977) can be approximated by

$$c \approx \sqrt{gH} \tag{5.28}$$

For a linearised, two-dimensional operator, the domain of dependence is now a characteristic cone, and thus this cone should lie within or on the region of interpolation of the surrounding points (Abbott & Basco, 1989), see figure (5.6).

Thus the CFL condition becomes

$$C_r = \frac{c}{\frac{\Delta s}{\sqrt{2}\Delta t}} < 1 \tag{5.29}$$

where Δs is the distance between two adjacent grid points in either spatial direction. Thus $\Delta s = \Delta x = \Delta y$. In the model $\Delta s = 50$ m and the sum of maximum depth of the bed below MLL and the free-surface elevation above the MLL at any time is 3 m. Thus $\Delta t < 7.4$ s. The double-sweep scheme, which is an implicit scheme, is stable for all values of C_r. However with Cr > 1, phase errors increase as the numerical waves move too slowly and thus the solution to the scheme becomes inaccurate.

The implementation of this Alternating Direction Implicit finite difference technique is discussed in the next chapter.

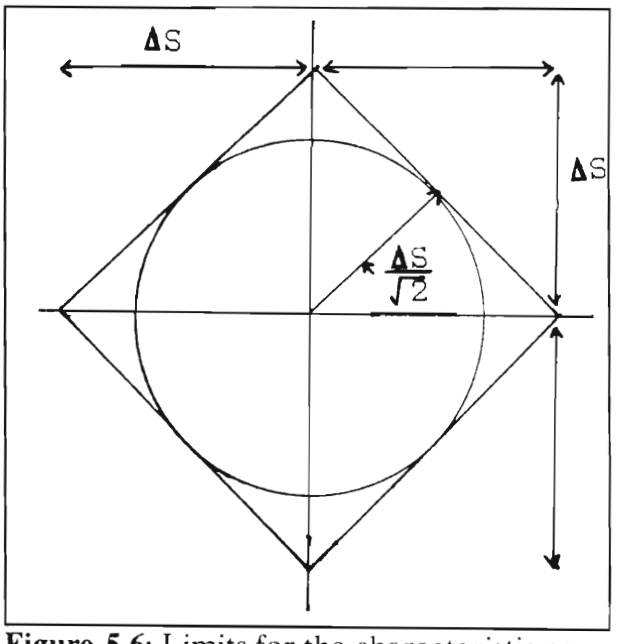

Figure 5.6: Limits for the characteristic cone for a two-dimensional operator

CHAPTER 6

COMPUTER SIMULATION

6.1 INTODUCTION

In this chapter the computer facilities available for the development of the hydrodynamic model will be specified; and the boundary conditions and results of two trial simulations will be discussed. The trial simulations are used to determine the areas where the model must be improved before it can be calibrated and used for the St Lucia Estuary.

6.2 THE COMPUTER PROGRAM

The hydrodynamic model was developed on an IBM compatible 80826 (without a numeric co-processor) and 640 KB memory. The programming language used was Turbo Pascal version 5.0.

The hydrodynamic equations are solved using a grid system to describe the variables at any spatial location throughout the estuary. At the centre of each grid cell the flow speed in both the x- and y-direction and the free-surface elevation above the MLL are specified, see figure (6.1). The centre of each cell will now be referred to as a datum point. These data are stored on the computer as a matrix with the same dimensions as the grid. In order to solve the hydrodynamic equations, a maximum of 16 matrices with these dimensions are required within the memory of the computer at any one time. For the simulations done in thesis, the grid dimensions were 11 x 33. The data can be stored in numerous data

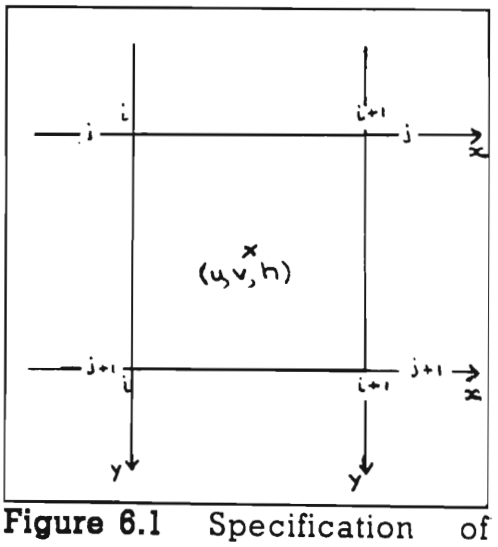

Figure 6.1 Specification of variables within the grid

types which depend on the range and number of significant digits which are stored. The variables which are specified in the simulation are real, thus they could be stored in the computer in any of the real types of data storage, two of which are 'real' and 'single', the former is 6 bytes in size and stores 11 significant digits and the latter is 4 bytes in size and stores 7 significant digits. Although, in the simulations done in this thesis, the computer would have sufficient memory to use either data type it was decided that 'single' would be used so that at any future stage estuaries with larger grid dimensions could be modelled without having to make any changes to the program. Also, due to the fact that the flow variables can only be measured accurately to within a couple of decimal places and that they are all within a small ranges, the flow velocity range is -1 $m.s^{-1}$ to 1 $m.s^{-1}$ and the free-surface elevation relative to the MLL range is -1 m to 1 m, the use of 11 significant digits is meaningless.

The computer model is split into two separate programs. The first, LOADALL, is used to input all the necessary initial data and boundary conditions. When executing LOADALL the following screen appears

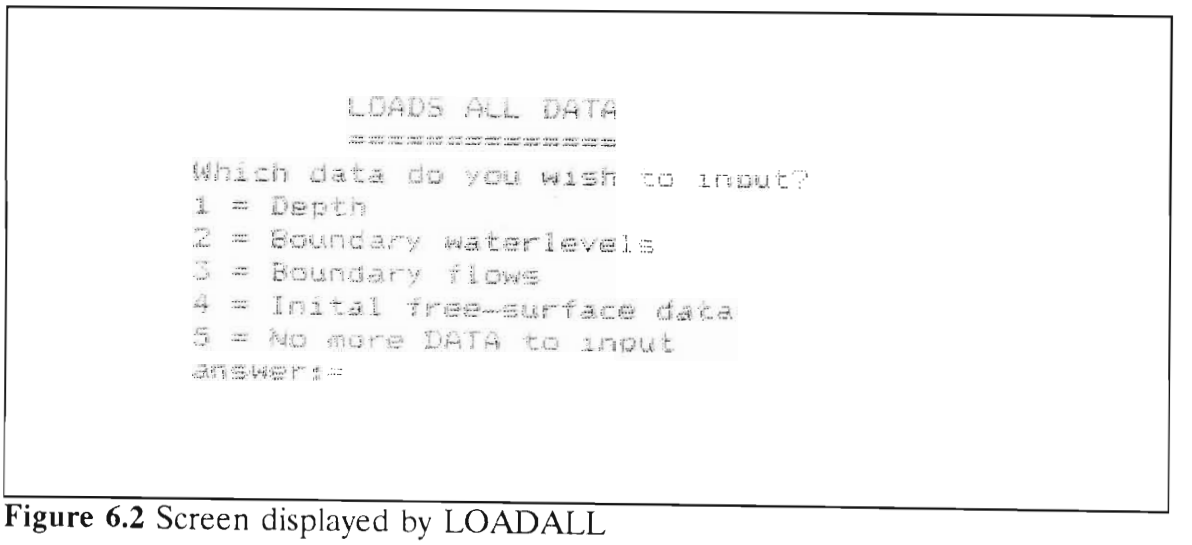

Figure 6.2 Screen displayed by LOADALL

Option 1 prompts the user to input the depth of the estuary bed below the Mean Lake Level (MLL) for all the data points. For the purpose of the simulations that have been done in this thesis the depth was specified at every alternate datum point in the x-direction and every 8^{th} datum point in the y-direction. The computer then used linear interpolation to calculate the remaining values. This was only done because the simulations were carried out using hypothetical data. A minor adjustment to the program would suffice for the input of all the real depth values.

Options 2 and 3 require the input of the variables which are needed to determine the boundary conditions at any given time as discussed in section 5.5.1 and 5.5.2.

Option 4 requires the input of the initial free-surface elevations relative to the MLL. The same method of data input is used as that used for the input of the depth of the bed below MLL.

At this stage the initial flow velocity for each datum point can be calculated by the method described in section 5.4.2.

Option 5 can be used at any stage to exit the program.

The second program SIMULATION performs the computer simulation. All constants, user defined data types, and global variables used by SIMULATION, are declared in the unit DSVAR1. The only way of changing these is by changing this unit. The duration for which the simulation is to run must also be preprogrammed in SIMULATION. Figure (6.3) is a flow chart for the program SIMULATION.

Two data sets, one at time **t = 0** and the next at **t = tm**, where **tm** is the size of the time step, are required to run the program. In the simulations done in this thesis, the data loaded in LOADALL is assumed to be that for **t = 0** and to get

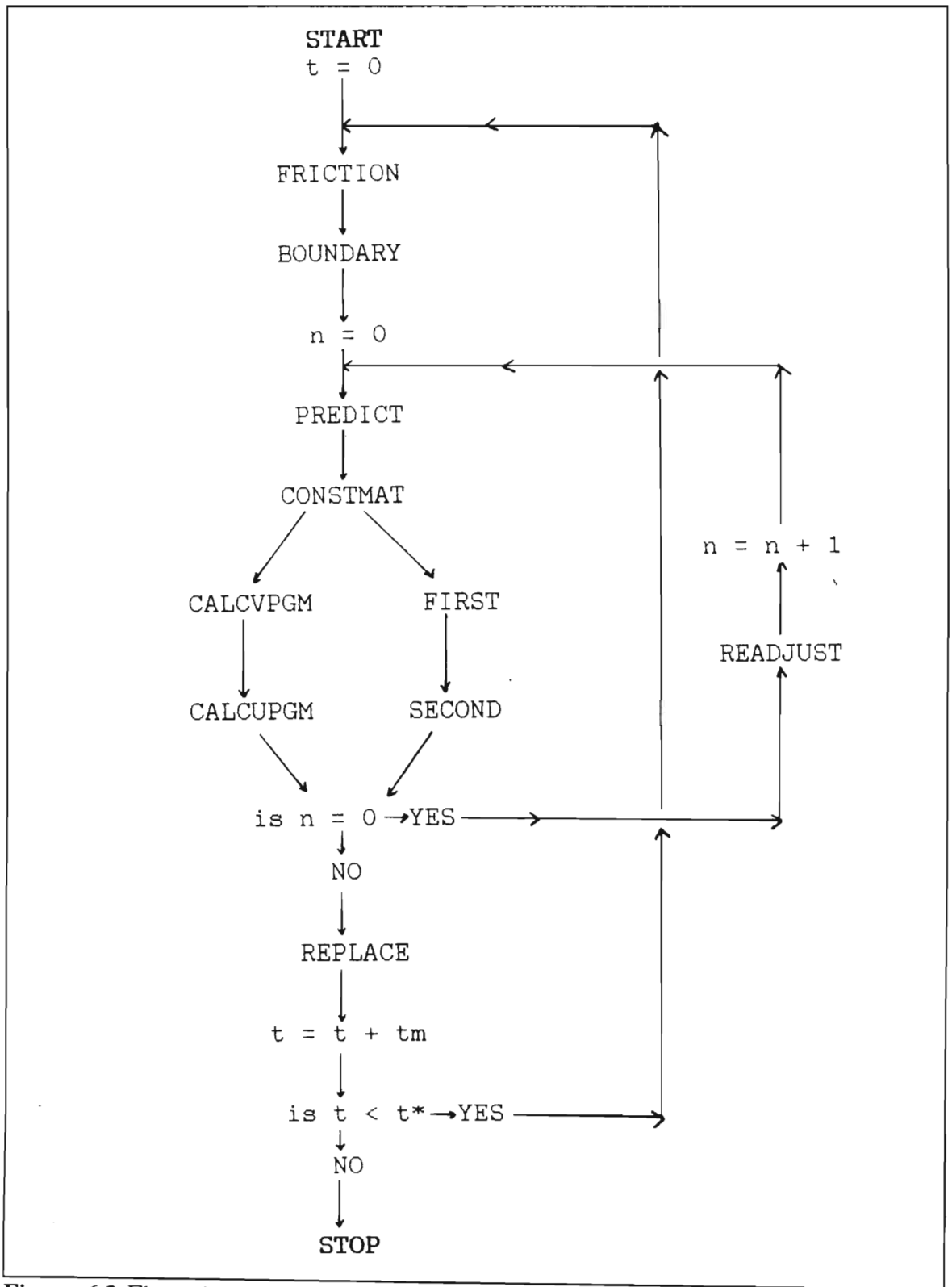

Figure 6.3 Flow chart for the program SIMULATION

the data necessary for **t = tm**, a constant value was added to the initial data. Although this method is not accurate, it suffices when the simulation is only being carried out for hypothetical data. For a simulation where accurate initial data is available, two different data sets would have to be entered.

The unit FRICTIONMAT generates the Chezy coefficient for each datum point. Although the absolute roughness is assumed to be constant, the hydraulic radius is continually changing as the free-surface elevation changes. Thus the friction matrix needs to be generated at each time step.

The unit BOUNDARY calculates the required boundary conditions as specified in section 5.5. As the time operator is split into two levels, the boundary conditions are calculated for both **t = tm + 1/2 tm** and **t = 2 tm**.

As discussed in section 5.2 the equations (4.20), (4.21) and (4.29) need to be linearised. This is done by predicting values of the flow velocity and free-surface elevation at **t = 2 tm**. Then using these predicted values and the values at **t = 0** and **t = tm,** approximate values for the flow velocity and free-surface elevation are generated for the duration of the time step. This process is done in unit PREDICT.

CONSTMAT generates the second terms in equations (5.4) and (5.5). These terms are constant throughout the complete iteration and thus this unit simplifies the program.

The unit CALCVPGM solves equation (5.5) explicitly, thus generating the flow speed in the y-direction at time **t = tm + 1/2 tm**. The unit FIRST performs the first implicit double sweep procedure on equations (5.4) and (5.6), thus generating the flow speed in the x-direction and the free-surface elevation at time **t = tm + 1/2 tm**.

The values of the flow variables at time **t = tm + 1/2 tm** are then used in the units CALCUPGM and SECOND. CALCUPGM solves equation (5.4) explicitly, thus generating the flow speed in the x-direction at **t = 2 tm**, while SECOND performs

the second double sweep procedure on equations (5.5) and (5.6) to generate the flow speed in the y-direction and the free-surface elevation at time **t = 2 tm**.

At this stage, the values of the flow variables that have been calculated for **t = 2 tm** and the values for **t = tm** are compared, and the values at **t = tm** are altered in order to give a better approximation to the real values. This is done as, initially, the data at time **t = tm** was generated by just adding a constant value at all data points throughout the estuary. The procedures from the unit PREDICT to SECOND are repeated. This repetition improves the original predictions and thus gives better approximations when the equations are linearised.

The final stage within the program is to change the data sets so that the data at **t = tm** now becomes the initial data set the data at time **t = 2 tm** becomes the second level data set. The process is repeated to calculate the flow variables at the next time **t = 3 tm.**

The simulation halts when the time for which the flow variables are being calculated exceeds some previously specified time, t^*.

6.2 DETAILS OF TWO SIMULATIONS PERFORMED

Two simulations of 120 seconds each were performed using the computer model, where the time step for each iteration was 2 seconds. The reason for the short duration of each simulation was, that at this stage, only hypothetical data were being used and the intention was only to check whether the model worked and to identify problem areas.

For the first simulation the initial time was taken as that time halfway between the high and low tides for the sea moving towards the low tide. In figures (5.4) and (5.5) this corresponds to the time **t = 0 s**. The second simulation was performed exactly half a tidal cycle later, or in other words the initial time was **t = 22320 s** in figures (5.4) and (5.5). For both simulations the same depth data were used, see figure (5.3).

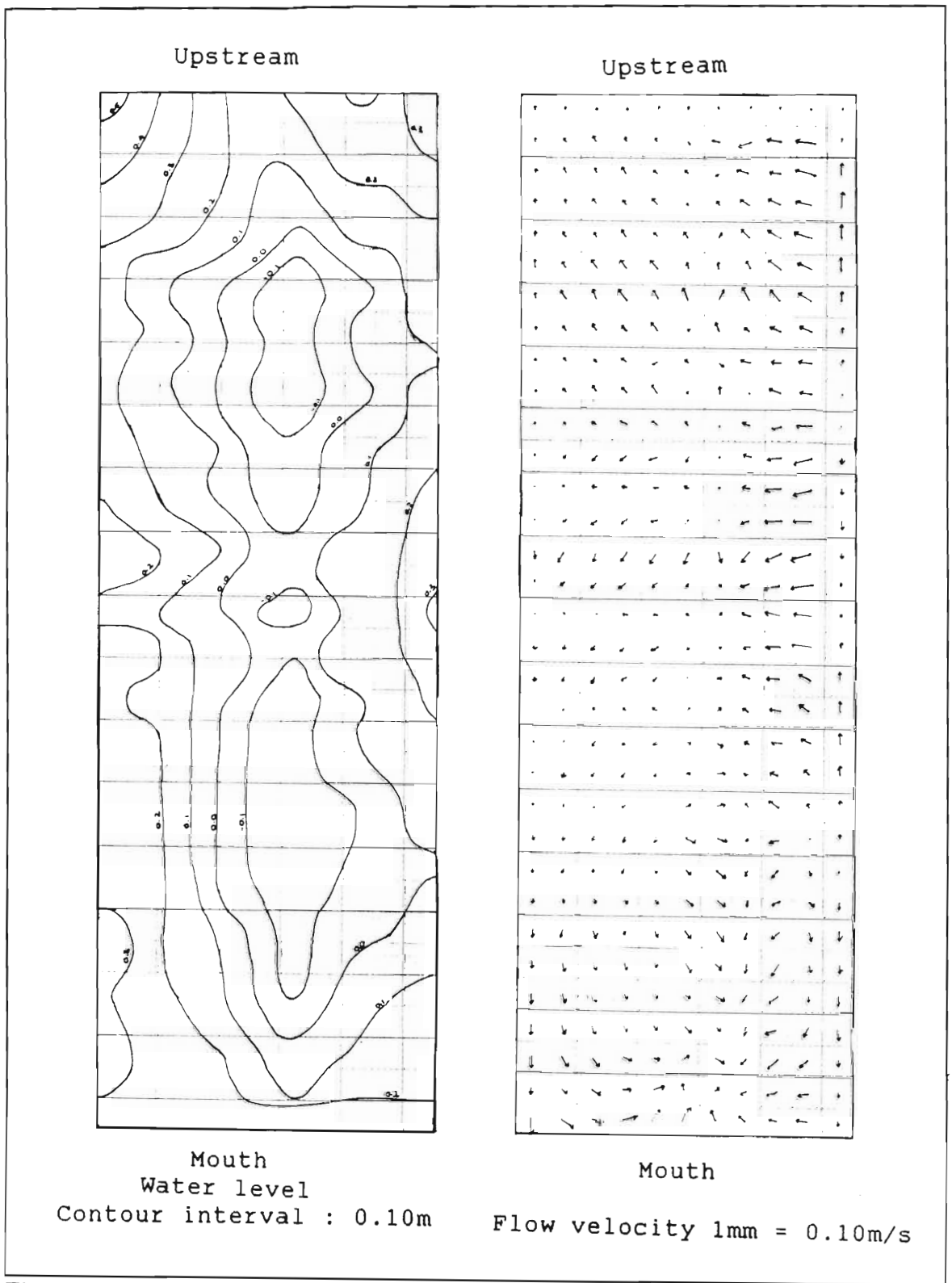

Figure 6.4 Results of the first simulation

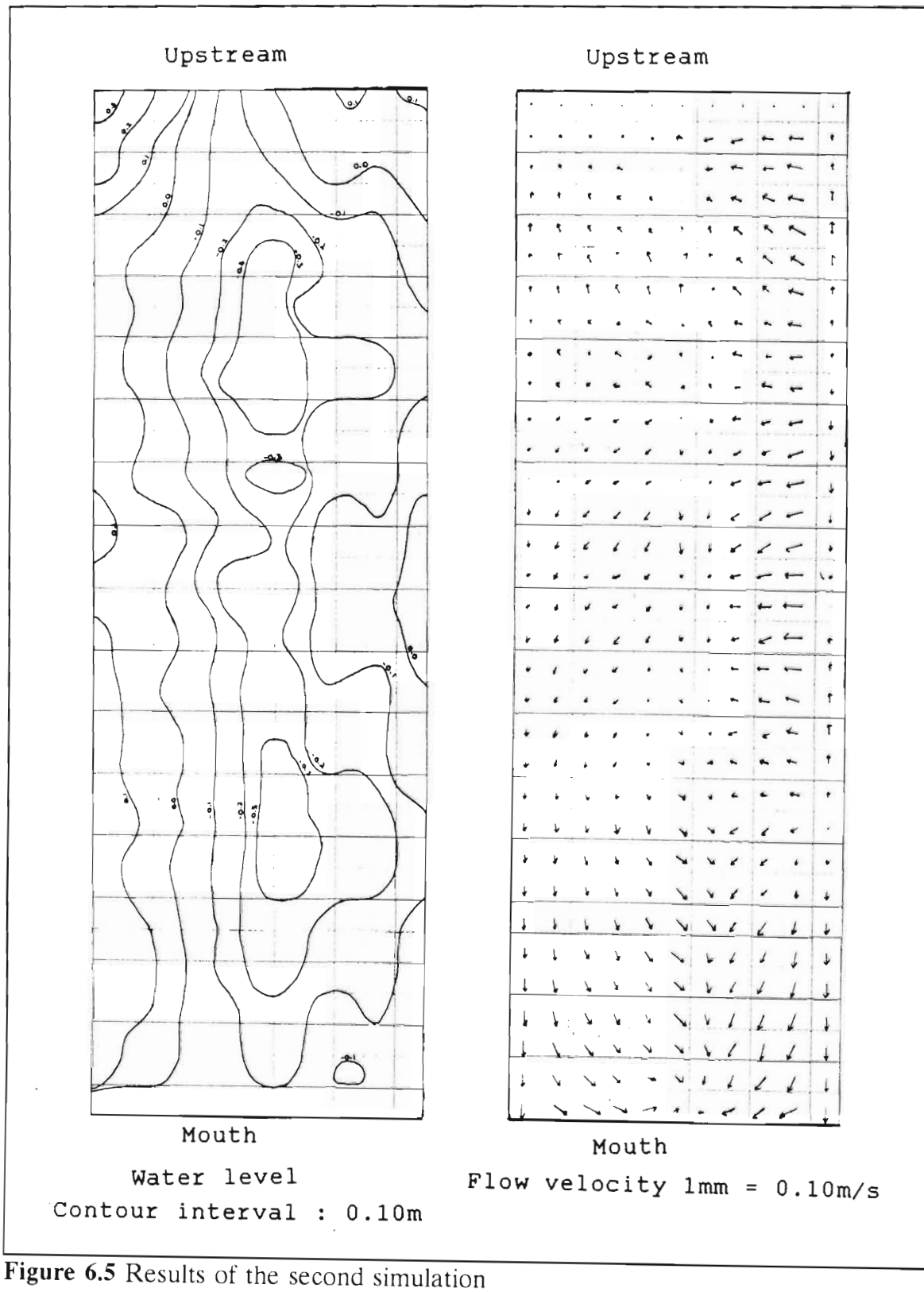

Figure 6.5 Results of the second simulation

Figures (5.4) and (5.5) show water levels and flow velocity values which were recorded during a spring tide on the 11 March 1989 by Anderson & Huizinga (1990). The maximum and minimum values for the flow velocity and water levels were halved in the simulations in order to approximate a tidal cycle mid way between spring and neap tide. The output for the first simulation can be seen in figure (6.4) and for the second simulation in figure (6.5). In the first simulation the initial flow velocity was predominantly into the estuary from the sea, or in other words in a westerly direction and in the second simulation the initial flow velocity was predominantly in a easterly direction.

A notable fact in the output of both simulations is that on the northern side of the estuary the flow velocity is great and directed towards the centre of the estuary. This could be as a result of the steeper slope of the estuary bottom on the northern side of the estuary as opposed to the southern side, see figure (5.3), or incorrect boundary conditions on the northern bank. In both cases this has resulted in a heaping effect of the water on the southern side of the estuary. It can also be seen that in the shallower regions of the estuary, the flow is generally less, and in the proximity of the ebb-tidal and flood-tidal channels the flow is greater. This emphasises the heaping effect on both the southern and northern sides of the estuary and the development of a relative trough over the channels.

In the first simulation, the flow should be in a westerly direction. However a reversal of the flow direction occurred in the eastern region of the estuary. Similarly, in the second simulation a reversal of the expected flow direction occurred in the westerly region of the estuary. There are a couple of possible causes for this phenomenon:

(1) the boundary conditions are not correct. Thus the in the first simulation the specified water levels at the eastern side of the estuary are not adequate to sustain the initial flow velocity in the westerly direction. Similarly, in the second simulation the flow velocity specified at the western side of the estuary is not great enough to counteract the initial pressure gradient which is acting in the opposing direction;

(2) due to the presence of ebb-tidal and flow-tidal channels, see figure (5.4), eddies are being formed. In both simulations the flow in the proximity of the channels is directed towards the channel centres.

A problem that is apparent in the results of both simulations is that the restriction of the flow parallel to the banks on the northern and southern boundaries is incorrect. As the flow velocity is specified at the centre of each grid cell, see figure (6.1), flow should be possible in the x-direction, only on the edge of the grid cell which forms the bank is flow in the x-direction impossible. However, to calculate what the flow velocity should be at these data points would require a vast amount of data. At present no such data have been collected. This problem also emphasises the heaping effects on the northern and southern sides of the estuary. Water can flow into these boundary regions from areas within the estuary. However once the water is in the boundary regions it can only be displaced in the y-direction. This accounts for the excessive heaping in the corners of the modelled area, especially the south-western and south-eastern regions.

Finally, the assumption that the absolute roughness, which is used in Chezy's coefficient, is uniform throughout the estuary is probably incorrect. The value for the absolute roughness was taken as that used by the Anderson & Huizinga (1990) for their one-dimensional model of the St Lucia estuary. Anderson & Huizinga (1990) altered the value of the absolute roughness in order to calibrate their model and thus it is possible that the value was not the correct value to have been used in the simulations performed in this thesis.

CHAPTER 7

DISCUSSION

Ultimately, a sediment transport model for estuarine environments is required by the Joint Venture Programme. As discussed earlier, for sediment transport to occur, a sediment source and a transporting medium, which is capable of initiating and sustaining transport, are needed. All sediment transport models which were reviewed in this thesis are dependent on the physical sediment properties. Thus, before a sediment transport model for an estuary can be developed, the following steps must be carried out:

(1) A study of the sediment types;
(2) A study of the sediment sources;
(3) A two-dimensional hydrodynamic model must be developed.

For the St Lucia Estuary, the first two steps have been completed by Wright (1990). This thesis has partially fulfilled the third step. The two-dimensional hydrodynamic model which has been developed in this thesis and applied to a hypothetical estuary, which is based on the St Lucia Estuary, still needs to be refined. However, to refine this model, a vast data collection programme must first be undertaken. The following sets of data, over several tidal cycles, are necessary to refine this model:

(1) the free-surface elevations relative to the Mean Lake Level (MLL) across the breadth of the mouth of the estuary;
(2) the flow velocities across the breadth of the estuary at the upstream boundary and close to both the banks;
(3) the size and extent of bed features throughout the estuary to improve the absolute roughness estimate;

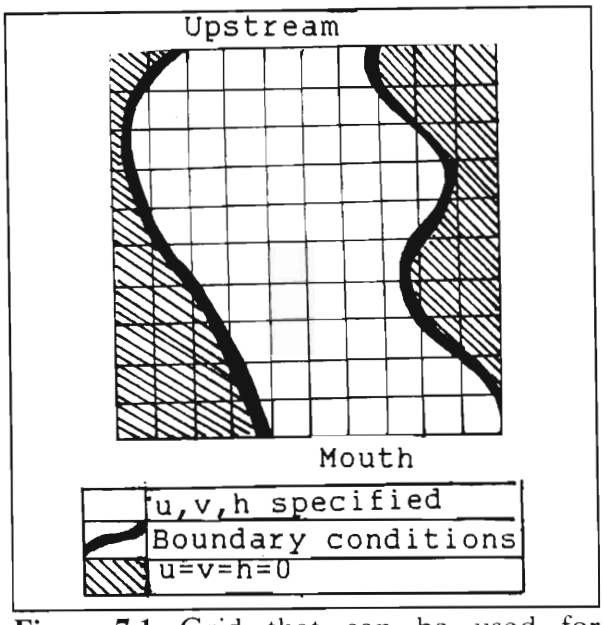

Figure 7.1 Grid that can be used for irregular shaped estuaries.

In its present form, the hydrodynamic model developed can be used on any estuary which can be approximated by a rectangular shape. Although it has not been done in this thesis, as the modelled region of St Lucia estuary is approximately rectangular, the model could be adapted in the following way so that it may be used for irregular shaped estuaries:

(1) a large rectangular grid is used so that the whole estuary falls within the grid area, see figure (7.1);

(2) for all points on the grid which lie outside the estuary, the depth of the bed below MLL,flow velocity, and the free-surface elevation relative to the MLL are also set at 0 for the duration of the iteration;

(3) the boundary conditions are the same as for the rectangular model. However, the program "realises" it has reached a boundary if the following or preceding grid point's depth below MLL is 0.

(4) once the program "realises" that it has reached the boundary, it must use different versions of equations (5.11) and (5.12), so that only the forward-difference operators that use values of the flow variables on the boundary, are not used.

The hydrodynamic model cannot cope with regions within an estuary that may become exposed during a tidal cycle. In order to develop a hydrodynamic model that is capable of coping with this, the exact locations and times during the tidal cycle at which the areas will be exposed, must be specified, and these must then be treated in a similar way to the boundary conditions.

For reasons discussed in section 4.3.1 the wind stress factor was not incorporated into this model. However, it could easily be included with only minor programming changes. The effect that the wind has on the wave energy cannot at present be included in the model.

Once this two-dimensional hydrodynamic model has been refined and calibrated for the St Lucia Estuary, the final stage in the development of a sediment transport model can begin.

REFERENCES

Abbott, M.B. & D.R. Basco (1989). Computational Fluid Dynamics. An Introduction for Engineers. Longman Scientific & Technical, London. 425 pp.

Ahilan, R.V. & J.F.A. Sleath (1987). Sediment Transport in Oscillatory Flow over Flat Beds. Journal of Hydraulics Division, ASCE, Vol 113, No. HY3, pp 308-322.

Allen, J.R.L. (1985). Principles of Physical Sedimentology. George Allen & Unwin, London. 272 pp.

Anderson, E.J & P. Huizinga (1990). One dimensional hydrodynamic and water quality model for the St Lucia estuary. Division of Earth, Marine and Atmospheric Science and Technology. CSIR Research Report no. 688. 81 pp.

ASCE Task Committee (1971). Sediment Transportation Mechanics: H. Sediment Discharge Formulas. Journal of Hydraulics Division, ASCE, Vol 97, No. HY4, pp 523-567.

Bagnold, R.A. (1956). Flow of cohensionless grains in fluids. Royal Soc London Philos. Trans. Vol 249 : pp 235-297.

Bagnold, R.A. (1960). Physics of Blown Sand and Desert Dunes. Methuen & Co. Ltd, London. 265 pp.

Bagnold, R.A. (1966). An Approach to the Sediment Transport Problem from General Physics. USGS Professional Paper 422-I. 37 pp.

Badenhorst, P. (1989). St. Lucia Dredging Monitoring. Interim Natal Parks Board Report No. 4: 4 pp.

Begg, G.W. (1978). The Estuaries of Natal. Natal Town and Regional Planning Report, 41: 657 pp.

Black, K.P. (1987). A numerical sediment transport model for application to natural estuaries, harbours and rivers. Numerical modelling : Applications to Marine Systems, J. Noye (ed), North-Holland: pp 77-105.

Chung, H.H. (1988). Fluvial Processes in River Engineering. John Wiley & Sons, New York. 432 pp.

Davis, J.M. (1976). The finite element method : an alternative subdomain method for modelling unsteady flow in coastal waters and lakes. Proc. International Symposium on unsteady flow in open channels, University of Newcastle-upon-Tyne, England. (April 12-15th, 1976): pp B41-B53.

Du Boys, P. (1879). Le Rhone et les Rivieres a Lit Affouillable. Annales des Ponts et Chaussees, Series 5, Vol 18: pp 141-195.

Einstein, H.A. (1942). Formulas for the Transportation of Bed Load. Trans. ASCE, Vol 107: pp 561-575.

Einstein, H.A. (1950). The Bed Load Function for Sediment Transportation in Open Channel Flows. U.S. Dept. Agriculture, Soil Consveration Services, Tech. Bull. 1026: 25 pp.

Huizinga, P. (1987). Computational aspects of the NRIO one-dimensional estuaries model. NRIO Memorandum 8703 : 9 pp.

Hutchison, I.P.G. (1976). Lake St. Lucia : mathematical modelling and evaluation of ameliorative measures. Report No. 1/76, Hydrological Research Unit, University of the Witwatersrand, Johannesburg: 347 pp.

James, W. (1968). Unsteady flow in open channels. Hydraulics notes issued by Div. Hydr. Engng., S. A. Inst. Civil Engineers. 24 pp.

James, W. & C.W.D. Horne (1969). Numerical computations of tidal propagation in the St. Lucia estuary. Trans. S. A. Inst. Civil Engineers, Vol 11: pp 323-326.

Laufer, J. (1954). The structure of turbulence in fully developed pipe flow. Natl. Advisory Comm. for Aeronautics Rept. 1174. 36 pp.

Leendertse, J.J. & S-K. Liu (1976). Three dimensional flow simulation in estuaries. Proc. International Symposium on unsteady flow in open channels, University of Newcastle-upon-Tyne, England. (April 12-15th, 1976): pp B11-B24.

Lyn, D.A. (1987). Unsteady Sediment Transport Modelling. Journal of Hydraulics Division, ASCE, Vol 113, No. HY1, pp 1-15.

McDowell, D.M. (1976). Modelling methods for unsteady flows. Proc. International Symposium on unsteady flow in open channels, University of Newcastle-upon-Tyne, England. (April 12-15th, 1976): pp B1-B10.

McDowell, D.M. & B.A. O'Connor (1977). Hydraulic Behaviour of Estuaries. The Macmillan Press Ltd, London. 102 pp.

Meyer-Peter, E & R. Muller (1948). Formulas for Bed-Load Transport. Report on Second Meeting of International Association for Hydraulic Research, Stockholm. pp 39-64.

Peaceman, D.W & H.H. Rachford (1955). The numerical solution of parabolic and elliptic differential equations. Journal of the Society of Industrial Applied Maths. Vol 3. 28 pp.

Reynolds, O. (1885). On the dilatancy of media composed of rigid particles in contact. Philos. Mag., 5th ser., Vol 20 : pp 469-489.

Rubey, W.W. (1933). Equilibrium conditions in debris-laden streams. Am. Geophys. Union Trans. 14th Ann. Meeting, pp 497-505.

Sauermann, H.B. (1966). Hydraulic model of St. Lucia Estuary. Transactions of the S. A. Inst. Civil Engineers. 8(4) : pp 126-134.

Simons, D.B. & F. Senturk (1976). Sediment Transportation Technology. Water Resources Publications, Colorado: 807 pp.

Strahler, A.N. & A.H. Strahler (1973). Environmental Geoscience: Interaction Between Natural Systems and Man. John Wiley & Sons, New York: 511 pp.

Swart, D.H. (1987). Erosion of Manmade Dune, Beachwood Mangrove Nature Reserve. CSIR Research Report, T/SEA 8713, 28 pp.

Task Committee on the Preparation of the Sedimentation Manual (1971). Sediment Transport Mechanics: H.Sediment Discharge Formulas. Journal of Hydraulics Division, ASCE, Vol 97, No. HY4, pp 523-567, April 1971.

Townsend, A.A. (1956). The structure of turbulent shear flow. Cambridge University press. 31 pp.

Van Heerden, I.L. & D.H. Swart (1986). An assessment of past and present geomorphological and sedimentary processes operative in the St Lucia Estuary and environs. Marine Geoscience and Sediment Dynamics Division, National Research Institute for Oceanology, CSIR Research Report no. 569. 105 pp.

Vanoni, V.A. (ed.) (1977). Sedimentation Engineering, ASCE Manuals and Reports on Engineering Practice.

Wright, C.I. (1990). The sediment dynamics of St. Lucia estuary mouth, Zululand, South Africa. Unpublished M.Sc. thesis, University of Natal, Durban : 160 pp.

Yalin, M.S. (1963). An Expression for Bed-load Transportation. Journal of Hydraulics Division, ASCE, Vol 89, No. HY3, pp 221-250.

Yalin, M.S. (1972). Mechanics of Sediment Transport. Pergamon Press: 290 pp.